

Coupled fluid flow with calc-silicate reactions around plutons: Results of numerical simulations

P.I. NABELEK

Dept. of Geological Sciences, University of Missouri,
Columbia, MO 65211, USA (nabelekp@missouri.edu)

Mineral assemblages in contact aureoles are the products of the interplay between heat and fluid flow that are induced by intrusion of magma into the upper crust. Metamorphism of calcareous shales causes metamorphic reactions that produce CO₂, which then becomes part of the hydrodynamic system. Flow of reactive H₂O-CO₂ fluids and progress of metamorphic reactions in an aureole of a granite pluton were simulated using a modified version of the US Geological Survey SUTRA code that allows calculation of metamorphic reactions in a transient P - T - XCO_2^{fluid} field. Several permeability structures of the aureole were considered, including: a) homogeneous, b) layered and c) reaction-enhanced. Reactions were assumed to occur only in horizontal calcareous shale beds. Magmatic, metamorphic, and sedimentary fluid sources were considered. The rates of reactions were assumed to be related to their ΔG 's at the prevailing P - T - XCO_2^{fluid} conditions at each node, an Arrhenian rate constant, and grain size.

Results show that after magma intrusion, overall fluid flow is away from the intrusion as the hydrostatic pressures in the inner aureole rise with temperature increase. Fluid composition in the inner aureole evolves rapidly toward high XCO_2^{fluid} as metamorphic reactions initiate before water begins to exsolve out of the pluton. Only after tremolite and diopside-forming reactions come to completion and local fluid pressures drop, infiltration of H₂O from the pluton becomes significant and can drive production of minerals such as wollastonite and vesuvianite. Further away from the intrusion, fluid composition initially reflects the CO₂ production in the inner aureole, and only later it is influenced by local reactions.

In the case of a homogeneous permeability structure of the aureole, fluid flux and composition are dispersed, while in a layered permeability structure, the highest fluid fluxes are confined to high permeability layers and fluid compositions remain discrete. When permeability increase is related to reaction progress, the highest fluid flux is confined to the inner aureole. The reaction-enhanced permeability model is in agreement with field and geochemical observations that suggest confinement of reactive fluid flow largely to inner calc-silicate contact aureoles.

Fate of ¹⁴C organic compounds released from sub-surface low-level radioactive waste repository

T. NAGAOKA^{1*}, N. YOSHIDA¹, T. NAKAMURA¹ AND
Y. MIYAUCHI²

¹Biotechnology Sector, Central Research Institute of Electric Power Industry (CRIEPI), Abiko, Chiba 270-1194, Japan
(*correspondence: nagaoka@criepi.denken.or.jp)
(t-nakam@criepi.denken.or.jp)

²Radioactive Waste Disposal Business Division, Japan Nuclear Fuel Limited (JNFL), Rokkasyo, Aomori, 039-3212, JAPAN (yoshihiro.miyauchi@jnfl.co.jp)

¹⁴C is a major radionuclide of concern in the sub-surface low-level radioactive waste disposal due to its long half-life (5730 years) and relatively high mobility in an aquifer. It is mainly released from the disposal site in the form of low-molecular-weight organic compounds such as acetate, acetaldehyde and ethanol that are generated abiogenically by Fischer-Tropsch reactions.

These low-molecular-weight organic compounds are degraded by anaerobic microorganisms in many subsurface environments and are therefore considered to be easily metabolized by indigenous microorganisms that alter the migration behavior of carbon-14 in an aquifer.

In the laboratory experiments, however, acetate was not anaerobically degraded by microorganisms indigenous to a pumice-tuff rock, even after incubation for at least 3 months; however, it was aerobically degraded to bicarbonate within a short period, i.e., 7 days. 16S rDNA analysis of the rock revealed clones related to the sulfate reducer, *Desulfovibrio* sp. and methanogens, *Methanosarcina* sp. and *Methanogenium frigidum*, indicating the possibilities of anaerobic microbial degradation of acetate in the subsurface environments. However, when growth media specific for sulfate reducers and methanogens were used, there was no evidence of anaerobic microbial degradation of acetate.

Because of the differences in the experimental conditions between the laboratory and aquifer environments, more definitive tracer test using ¹³C-labeled acetate is now used to analyze its bioavailability at a site in Rokkasyo, Japan.

Diffusion-modified volatile contents in melt inclusions: Evidence for open system behaviour

A.N. NAGLE¹, A.M. KOLESZAR², A.E. SAAL¹, Y. LIANG¹,
E.H. HAURI³ AND M. D. KURZ⁴

¹Brown University, Department of Geological Sciences,
Providence, RI, USA (Ashley_Nagle@brown.edu)

²Oregon State University, Department of Geosciences,
Corvallis, OR, USA

³Department of Terrestrial Magnetism, Carnegie Institution of
Washington, Washington, DC, USA

⁴Woods Hole Oceanographic Institute, Woods Hole, MA,
USA

Melt inclusions are assumed to be isolated post-entrapment, and therefore are considered ideal for determining the primitive concentration of volatile elements in magmas. Ratios of volatile to similarly incompatible non-volatile elements (H₂O/Ce, F/Nd, etc.) are used to identify processes (e.g. degassing) that decouple volatile concentrations from other refractory incompatible trace elements (ITEs).

We recently performed major, trace and volatile analyses on melt inclusions and their olivine hosts in basalts from the island of Fernandina in the Galápagos Archipelago. These data show that ratios of volatile/non-volatile elements vary significantly for ITE-depleted and ITE-enriched melt inclusions from the same host basalt. Strongly ITE-depleted lavas have very high H₂O/Ce and F/Nd ratios, with H₂O and F concentrations similar to the ITE-enriched host glass. These data suggest that the melt inclusions were modified post-entrapment by diffusion of H₂O and F from the surrounding ITE-enriched melt, through the host olivine, and into the melt inclusion. However, none of the host olivines have Mg#’s that are in equilibrium with the composition of the host basalt.

The different timing required for diffusive re-equilibration of H₂O, F and Fe-Mg between the melt inclusion, olivine and host glass provides a unique opportunity to investigate the time-scales of magma ascent post-entrapment of the melt inclusions. Our data suggest that water, which is a fast diffusing element, has equilibrated with the external melt while comparatively slower diffusing elements (like Fe-Mg) have not. The difference in the extent of equilibration will be used to place constraints on the time between melt inclusion entrapment and eruption for the Fernandina lavas.

Constraining hinterland tectonics and basin evolution from the detrital record: A multi-technique approach applied to sediments in the Bengal Basin, Bangladesh

Y. NAJMAN^{1*}, S. AKHTER², R. ALLEN¹, S. ANDO³,
M. BOUDHAGER-FADEL⁴, M. BICKLE⁵, A. CARTER⁴,
E. CHISTY⁶, E. GARZANTI³, G. OLIVER⁷, R. PARRISH⁸,
M. PAUL⁹, L. REISBERG⁹, G. VEZZOLI³, J. WIJBRANS¹⁰
AND E. WILLET¹¹

¹Lancaster Univ, UK

(*correspondence: y.najman@lancs.ac.uk)

²Dhaka Univ, Bangladesh

³Univ Milano-Bicocca, Italy

⁴UCL, UK

⁵Cambridge Univ, UK

⁶Cairn Energy, Bangladesh

⁷St. Andrews Univ, UK

⁸NIGL, UK

⁹CNRS-CRPG Nancy, France

¹⁰Vrije Univ, Netherlands

¹¹Cairn Energy, UK

The application of isotopic analyses to detrital material, in particular techniques applied to single grains, has revolutionised the utility of the detrital record to determination of hinterland tectonics and basin palaeogeography and evolution. Using the sediment record to constrain hinterland tectonism is of particular value where the bedrock record is overprinted by later metamorphism, or removed by tectonism or erosion. Now a plethora of techniques are available and a multi-proxy approach is preferable if provenance is to be constrained robustly.

We applied 11 techniques to the Tertiary sediments of the Bengal Basin, in order to understand the tectonic and erosion history of the Himalaya, and to constrain the evolution of this petroliferous basin. The principle objective of the study was to search for the earliest record of Himalayan erosion, as the Paleogene archive of orogenic erosion is scant. We used seismic data to determine sediment input direction, biostratigraphic and isotopic methods to constrain formation ages, and petrographic, heavy mineral, and a number of geochemical and isotopic techniques (including Ar-Ar, U-Pb, fission track, Sm-Nd and Re-Os) to determine that by 38 Ma, sediments are Himalayan rather than Indian craton or Burman derived. Comparison between detrital mineral ages and sediment depositional age determined by biostratigraphy indicates rapid exhumation of the orogen at this time

Our data reduce the time gap between collision and known onset of erosion from the southern flanks of the east-central Himalaya from >20 Myrs to 12 Myrs. This has implications for models of crustal deformation and tectonic-erosion coupling, as well as the proposed influence of Himalayan erosion on Cenozoic global cooling and the marine Sr record

Precise Mo isotopic analysis on Pacific and Antarctic seawater

Y. NAKAGAWA^{1*}, M. L. FIRDAUS¹, K. NORISUYE¹,
Y. SOHRIN¹, K. IRISAWA² AND T. HIRATA²

¹Institute for Chemical Research, Kyoto University, Uji,
Kyoto, 611-0011, Japan

(*correspondence: ynakagawa@inter3.kuicr.kyoto-u.ac.jp)

²Tokyo Institute of Technology, 2-12-1 O-okayama,
Meguro-ku, Tokyo, 152-8551, Japan

In Mo isotopic geochemistry, Mo isotopic ratio data for the seawater is very important as a standard reference value. However, mainly due to analytical difficulty in precise isotopic ratio measurement, only few data have been reported for the seawater samples [1, 2]. Moreover, the reported isotopic ratio data varied significantly, and probably was possessed with low reliability. To overcome this, we have developed a new preconcentration technique using a chelating resin TSK-8HQ column for the precise isotopic ratio measurement with a MC-ICP-MS (Nu Plasma 500). The mass-discrimination effect was externally corrected by an exponential law using the ⁸⁸Sr/⁸⁶Sr ratio. In order to evaluate the small changes in the resulting Mo isotopic ratio data, the sample-standard bracketing technique was employed. Combination of the new chemical preconcentration technique and the correction techniques enabled us to obtain accurate and precise Mo isotopic ratio data for the seawater.

We applied the proposed method to seawater samples collected from 5 sampling stations in the Pacific Ocean that ranged from subarctic to subtropical regions. They included samples of four water masses: the Pacific Deep Water, North Pacific Intermediate Water, Western North Pacific Central Water and Pacific Subarctic Water. The salinity normalized (S = 35) mean Mo concentration (n = 108, excluding 5 outlier) was 10.4 ± 0.5 ppb (2 s.d.). The mean δ^{98/95}Mo (n = 107, excluding 2 outlier) was 2.47 ± 0.09 (2 s.d.), demonstrating that the Mo concentrations and isotopic compositions were uniform among different water masses, depths and sampling stations. Although the observation of Mo isotopic fractionation through active biological nitrogen fixation could be expected at subtropical area, we did not find significant change in Mo concentrations and isotopic compositions in seawater by the biological activity. We are going to analyze seawater samples from the Antarctic Ocean, and report the Mo isotopic data obtained as well.

[1] Barling *et al.* (2001) *EPSL* **193**, 447-457. [2] Siebert *et al.* (2003) *EPSL* **211**, 159-171.

Serpentinized olivine-rich gabbros near the Kairei Hydrothermal Field, Central Indian Ridge: A key to understanding the unique chemistry of the vent fluid

KENTARO NAKAMURA¹, TOMOAKI MORISHITA²,
KEN TAKAI³, KAORI HARA² AND HIDENORI KUMAGAI¹

¹Institute for Research on Earth Evolution (IFREEE), Japan
Agency for Marine-Earth Science and Technology
(JAMSTEC), Yokosuka, Japan (kentaron@jamstec.go.jp,
kumagai@jamstec.go.jp)

²Graduate School of Natural Science and Technology,
Kanazawa University, Kanazawa, Japan
(moripta@kenroku.kanazawa-u.ac.jp,
kaori-h@earth.s.kanazawa-u.ac.jp)

³Subground Animalcule Retrieval (SUGAR) Program, Japan
Agency for Marine-Earth Science and Technology
(JAMSTEC), Yokosuka, Japan (kent@jamstec.go.jp)

The Kairei Hydrothermal Field (KHF) on the first segment of the Central Indian Ridge is known to be characterized by an unusually high concentration of H₂ in the vent fluids [1]. Recently, much attention has been paid to the KHF, because the H₂-rich hydrothermal fluids are known to host a hydrogen-based hyperthermophilic subsurface lithoautotrophic microbial ecosystem, which is considered to be a likely modern proxy for the early Earth ecosystems prior to photosynthesis [2]. Despite the increasing interest in the fluid chemistry and associated biota of the KHF, however, the cause of the unique chemistry of the hydrothermal fluids is still unclear [3].

Here, we report the discovery of serpentinized olivine-rich gabbros from a small ocean core complex (OCC) at 15 km east of the KHF. Dives with the manned submersible *Shinkai 6500* recovered plagioclase-dunite, troctolite, and olivine gabbro samples from the OCC. Although these rocks are not typical mantle peridotite which is well known as a host of H₂-rich hydrothermal vent fluids, all the samples have been subjected to serpentinization to various extents. Microscopic observation revealed that the olivines in the samples were replaced by serpentine + magnetite, indicating the generation of H₂ by the serpentinization reaction. The results of the geological and petrological investigations suggest that the hydrothermal serpentinization of the olivine-rich gabbros is responsible for the unusually high concentration of H₂ in the Kairei hydrothermal fluids driving the occurrence of the unique microbial ecosystem.

[1] Van Dover *et al.* (2001). [2] Takai *et al.* (2006).
[3] Gallant & Von Damm (2006).

Presolar organic globules in astromaterials

K. NAKAMURA-MESSENGER^{1*}, S. MESSENGER²,
L.P. KELLER², S.J. CLEMETT¹ AND M.E. ZOLENSKY³

¹ESCG/NASA Johnson Space Center, Houston, TX 77058

USA (keiko.nakamura-1@nasa.gov,
simon.j.clemett@nasa.gov)

²Code KR, NASA Johnson Space Center, Houston, TX 77058

USA (scott.r.messenger@nasa.gov,
lindsay.p.keller@nasa.gov)

³Code KT, NASA Johnson Space Center, Houston, TX

Presolar grains were identified in meteorite residues 20 years ago based on their exotic isotopic compositions [1]. Their study has provide new insights into stellar evolution and the first view of the original building blocks of the solar system. Organic matter in meteorites and IDPs is highly enriched in D/H and ¹⁵N/¹⁴N at μm scales, possibly due to presolar organic grains [2-4]. These anomalies are ascribed to the partial preservation of presolar cold molecular cloud material. Identifying the carriers of these anomalies and elucidating their physical and chemical properties may give new views of interstellar chemistry and better understanding of the original components of the protosolar disk. However, identifying the carriers has been hampered by their small size and the inability to chemically isolate them.

Thanks to major advances in nano-scale analytical techniques and advanced sample preparation, we were able to show that in the Tagish Lake meteorite, the principle carriers of these isotopic anomalies are sub- μm , hollow organic globules [5]. The organic globules likely formed by photochemical processing of organic ices in a cold molecular cloud or the outermost regions of the protosolar disk [5].

Organic globules with similar physical, chemical, and isotopic properties are also recently found from Bells CM2 carbonaceous chondrite, in IDPs [6] and in the comet Wild-2 samples returned by Stardust [7]. These results support the view that microscopic organic grains were widespread constituents of the protoplanetary disk. Their exotic isotopic compositions trace their origins to the outermost portions of the protosolar disk or a presolar cold molecular cloud.

[1] Zinner in *Treatise on Geochemistry* (2004) pp. 17-39.

[2] Messenger (2000) *Nature* **404**, 968. [3] Busemann *et al.*

(2006) *Science* **312**, 727 [4] Floss *et al.* (2004) *Science* **303**,

1355. [5] Nakamura-Messenger *et al.* (2006) *Science* **314**,

1439. [6] Messenger *et al.* (2008) *LPSC XXXIX*, #2391

[7] Matrajt *et al.* (2007) *MAPS* **42**, 5138.

Multiple Sulfur isotope fractionation of SO₂ by UV radiation with narrowly-defined wavelengths

HIROSHI NARAOKA^{1*} AND SIMON R. POULSON²

¹Kyushu Univ. Fukuoka 812-8581, Japan

(*correspondence: naraoka@geo.kyushu-u.ac.jp)

²Dept. Geol. Sci. & Eng. MS172, Univ. Nevada-Reno, Reno,

NV, 89557-0138, USA (poulson@mines.unr.edu)

Mass-independent fractionation of sulfur (MIF-S) isotopes in Archean sedimentary rocks has been used to indicate a very low O₂ pressure in the Earth's early atmosphere, as large MIF-S can be experimentally produced by UV photolysis of SO₂ in an atmosphere free of O₂ and O₃ [1]. In this study, we have measured the UV absorption spectra of the four pure sulfur isotopomers of SO₂ (³²SO₂, ³³SO₂, ³⁴SO₂, and ³⁶SO₂) to reveal an isotope-dependent spectral shift at UV wavelengths.

In order to investigate the interaction between UV photolysis of SO₂ and the spectral shift, we have studied SO₂ photolysis by 193 nm and 213 nm lasers. Degradation of SO₂ is a first-order reaction, such that $-d[\text{SO}_2]/dt=k[\text{SO}_2]$, where k is the rate constant. It is likely that k is proportional to the absorption cross section of SO₂. At 193 nm, the cross sections are quite different for the four sulfur isotopomers. Using the spectral data, $\delta^{33}\text{S}$, $\delta^{34}\text{S}$ and $\delta^{36}\text{S}$ values of residual SO₂ after UV photolysis can be calculated, and these values show good agreement with the measured values [1]. In contrast, at 213 nm there is little difference in the cross sections of the sulfur isotopomers, which is consistent with essentially zero MIF-S produced by 213 nm photolysis. Hence, the large MIF-S produced by SO₂ photolysis using UV lasers or resonance lamps is a result of the interaction of the narrowly-defined UV wavelengths emitted by these light sources with the isotope-dependent UV absorbance of the SO₂ isotopomers. In turn, this suggests that Archean MIF-S signatures may not necessarily indicate low O₂ concentrations in the Archean atmosphere.

[1] Farquhar *et al.* (2001) *JGR* **106**, 32829.

Alpha-radiation damage in diamond

L. NASDALA^{1*}, A.M. GIGLER², M. WILDNER¹,
D. GRAMBOLE³, A.M. ZAITSEV⁴, J.W. HARRIS⁵,
W. HOFMEISTER⁶, H.J. MILLEDGE⁷ AND S. SATITKUNE⁶

¹Institut für Mineralogie und Kristallographie, Universität
Wien, Althanstr. 14, A-1090 Wien, Austria

(*correspondence: lutz.nasdala@univie.ac.at)

²Sekt. Kristallographie, LMU, D-80333 München, Germany

³FZ Dresden-Rossendorf, D-01328 Dresden, Germany

⁴CUNY, Staten Island, NY 10314, USA

⁵University of Glasgow, Glasgow G128QQ, UK

⁶Johannes Gutenberg-Universität, D-55099 Mainz, Germany

⁷University College London, London WC1E 6BT, UK

We studied both the extent and distribution of structural damage in diamond crystals that was generated through either natural or artificial irradiation with alpha particles (i.e. He²⁺ ions with energies in the MeV range), and the related formation of colour-centres. A range of non-destructive micro-techniques was applied. At high irradiation doses $\geq 10^{16}$ ions per cm², diamond may be transformed locally into an amorphous state (maximum damage generated at the far ends of helium trajectories). The resulting volume expansion causes compressive strain in the neighbouring (crystalline) diamond, detected by an upshift of the diamond LO=TO Raman band [1, 2]. This volume expansion is why radiation-damaged spots at the surface of natural diamond crystals often have an up-domed shape.

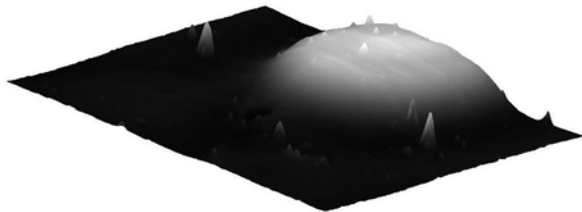


Figure 1: Topography (AFM scan) of the surface of a diamond from Namaqualand, R.S.A. The radiation-damaged spot is seen as a broad hump (diameter $\sim 36 \mu\text{m}$, height $\sim 400 \text{ nm}$); small peaks are artefacts (dust particles at the surface).

Visible radiation-induced green colouration of diamond (mainly caused by a broad absorption band at $\sim 16000 \text{ cm}^{-1}$ assigned to the GR1 centre) is generated at moderate doses of 10^{14} – 10^{15} He ions per cm² [3]. This irradiation resulted in a lowly damaged state (maximum damage $\leq 0.005 \text{ dpa}$).

[1] Hanfland *et al.* (1985) *Phys. Rev.* B31, 6896-6899.

[2] Nasdala *et al.* (2005) *Am. Mineral.* **90**, 745-748. [3] Vance *et al.* (1973) *Miner. Mag.* **39**, 349-360.

Helium-Ne-Ar systematic in Lena Trough lavas, Arctic Ocean

F. NAURET¹, M. MOREIRA¹ AND J.E. SNOW²

¹Institut de Physique du Globe de Paris, Laboratoire de
Géochimie et Cosmochimie, 4 pl. Jussieu, 75005 Paris,
France (nauret@ipgp.jussieu.fr)

²University of Houston, Departement of Geosciences,
Houston, TX, 77204

Lena Trough is considered as a non-volcanic continental rift in the Arctic Ocean. Nevertheless, rare volcanic rocks dredged at 3500 m deep in the southern Lena Trough are alkali-rich lavas with SiO₂ > 51%, Al₂O₃ > 18% and K₂O $\sim 2 \text{ wt\%}$. Based Sr-Nd-Hf-Pb isotopes, these lavas are interpreted as reflecting a binary mixing between a depleted MORB mantle component and a garnet non-peridotitic fertile component derived [1]. Furthermore, these lavas display a DUPAL-like anomaly. In order to test the binary mixing scenario and the origin of the Arctic DUPAL anomaly, we have measured concentrations and isotopic ratios of He, Ne, and Ar by step crushing. Lena Trough lavas display ⁴He/³He between 89,650 and 96,860 similar to the mean MORB ratio. Neon isotope ratios display values from 10.08 to 11.04 for ²⁰Ne/²²Ne and from 0.029 to 0.0434 for ²¹Ne/²²Ne. The samples fall on the MORB line. ⁴⁰Ar/³⁶Ar vary from 349 to 6964, lower than the MORB mantle value of $\sim 27,000$ suggesting the presence of an atmospheric component (air contamination or mantle-derived). Samples have typical MORB helium compositions and the fertile component is not detected with He. This distinguishes the Arctic from the south hemisphere DUPAL anomalies where radiogenic helium ratios were measured. The fertile component is therefore considered either as strongly degassed in helium before mixing or as young or/and U-Th depleted. Origin of this fertile component will be discussed in the light of He-Ne-Ar systematic.

[1] Nauret, F., J.E. Snow, and D. Weis, *J. Petrol.*, submitted.

Evolution of micro-porosity during weathering of basalt

A. NAVARRE-SITCHLER¹, D. COLE², G. ROTHER² AND S. BRANTLEY³

¹Department of Geosciences, Penn State University, University Park, PA (akn112@psu.edu)

²Oak Ridge National Laboratory, Oak Ridge, TN coledr@ornl.gov (rotherg@ornl.gov)

³Earth and Environmental Systems Institute, Penn State University, University Park, PA (brantley@essc.psu.edu)

In hydrology and geochemistry, porosity is arguably the most important physical property of a rock because it provides pathways for water flow or infiltration. Chemical reactions induce changes in porosity that change the rates of fluid transport and thus potentially the overall rates of reaction. We investigated porosity evolution during weathering rind formation on basalt clasts. Micro-computed tomography was used to evaluate changes in porosity with weathering down to pore sizes of ~4 μm and reactive transport models were developed that demonstrate the importance of porosity evolution in this system. Small-angle (SANS) and ultra small-angle neutron scattering (USANS) data extend our investigation of porosity evolution during weathering down to nanometer size pores.

SANS and USANS data were collected across the weathering interface of the basalt clasts at the Center for Neutron Research (NIST). The scattering intensity increases by one order of magnitude from the unweathered to weathered samples. Bulk chemical data from electron microprobe analyses and hydrogen concentrations determined using prompt-gamma neutron activation analysis were used to evaluate changes in chemical composition and thus scattering length density with weathering.

To investigate pore distribution we examine scattering curves for each of the samples where scattering intensity is plotted as a function of scattering angle (q) on a log-log plot. The fractal nature of these rocks is assessed using the slope of data plotted on the scattering curves. We observe that the fractal nature of the pore system in rocks previously observed is maintained during weathering. A constant slope of -3.3 is observed over the entire range studied (approx. 1nm -5 μm) in the unweathered basalt and we use a surface fractal model to interpret these results. Scattering data from the weathered basalt show a break in slope. A slope of -3.3 is observed in the high q region but a slope of -2.6 is observed in the low q region. This indicates the presence of surface fractality at nanometer length scales and mass fractality in the micron range for weathered basalt.

Size-driven structural and thermodynamic complexity in Iron oxides

ALEXANDRA NAVROTSKY^{1*}, LENA MAZEINA¹ AND JURAJ MAJZLAN²

¹Peter A. Rock Thermochemistry Laboratory and NEAT ORU, University of California at Davis, Davis, CA 95616 USA (*correspondence: anavrotsky@ucdavis.edu)

²Institute of Mineralogy and Geochemistry, Alberstraße 23b, Albert-Ludwig University, D-79104 Freiburg, Germany

Iron oxides occur ubiquitously in environmental, geological, planetary, and technological settings. They exist in a rich variety of structures and hydration states. They are commonly fine grained (nanophase) and poorly crystalline. This review summarizes very recently measured thermodynamic data for their formation and surface energies. These data are essential to calculate the thermodynamic stability fields of the various iron oxide and oxyhydroxide phases and understand their occurrence in natural and anthropogenic environments. The competition between surface enthalpy and the energetics of phase transformation leads to the general conclusion that polymorphs metastable as micrometer-sized or larger crystals can often be thermodynamically stabilized at the nanoscale. Such size-driven crossovers in stability help explain patterns of occurrence of different iron oxides in nature.

Cl-rich phlogopite-celadonite mica: Synthesis, X-ray study and petrological implication

SABRINA NAZZARENI¹, OLEG SAFONOV²,
PAOLA COMODI¹ AND LUCA BINDI³

¹Department of Earth Sciences, University of Perugia, Italy
(sabrina.nazzaren@unipg.it)

²Institute of Experimental Mineralogy, Chernogolovka,
Institutskaya str., 4, 142432 Russia (oleg@iem.ac.ru)

³Museo di Storia Naturale, Sezione di Mineralogia, Università
di Firenze, Via La Pira 4, I-50121, Firenze, Italy

Unique high-Si micas, phlogopite-Al-celadonite solid solutions, are associated with inclusions of alkalic Cl-bearing carbonate-silicate and chloride-carbonate liquids [1, 2, 3] in diamonds from kimberlites of Africa, Canada, and Yakutia. Micas coexisting with omphacites and KCl-rich brines in diamonds show high Cl content [1].

We produced Si-rich Cl-bearing mica as accessory phase in the join $\text{CaMgSi}_2\text{O}_6\text{-NaAlSi}_2\text{O}_6\text{-KCl}$ at 4 GPa and 1250-1200°C. It coexists with diopside-jadeite pyroxene, K-rich Cl-bearing aluminosilicate glass and/or sanidine, as well as with (K,Na)Cl. Micas show negative correlation between tetrahedral Si and octahedral (Al+Mg), that corresponds to a substitution $\text{Al}^{\text{T}} + (\text{Mg} + \text{Al})^{\text{M}} \Leftrightarrow 2\text{Si}^{\text{T}} + \text{v}^{\text{M}}$. In addition, Cl positively correlates with Si. X-ray diffraction study of a single mica crystal of composition $\text{K}_{1.01}(\text{Mg}_{2.45}\text{Al}_{0.19}[\]_{0.35})(\text{Si}_{3.52}\text{Al}_{0.48})\text{O}_{10}[(\text{OH},\text{O})_{1.66}\text{Cl}_{0.34}]$ (C2/m, 1M polytype, $a = 5.299(4)$ Å, $b = 9.167(3)$ Å, $c = 10.226(3)$ Å, $\beta = 100.06(4)^\circ$, $V = 489.1(4)$ Å³) shows that the major crystal chemical factor controlling incorporation of Cl in the mica structure is the tetrahedral rotation angle, which is much lower (2.58°) than that of phlogopite. Thus, the tetrahedral ring is almost hexagonal, resulting in a large interlayer cavity that favors the entry of Cl instead of OH.

Our experimental and crystal structural data support miscibility between di- and tri-octahedral micas at high pressures. The Si-rich micas are indicators of K and Cl activity in the diamond-forming media: K extracts Al from phlogopite to the melt, pressure stabilizes the phlogopite-celadonite solid solution, and allows incorporation of Cl.

The study is supported by the RFBR (07-05-00499), the RF President Grant MD-130.2008.5, the RAS Project P-9-3.

[1] Izraeli E.S., Harris J.W., Navon O. (2004) *Geochim. Cosmochim. Acta* **68**, 2561-2575. [2] Klein-BenDavid O., Wirth R., Navon O. (2006) *Am. Mineral.* **91** 353-356. [3] Shatsky V.S., Ragozin A.L., Zedgenizov D.A. (2007) *Lithos* (in press)

Microbial sensing of, and interaction with, metal oxides and other solid surfaces

K.H. NEALSON

University of Southern California, Los Angeles, CA, USA
(knealson@usc.edu)

One of the hallmarks of microbial metabolism (probably of all metabolism) is the need for electron flow. Substrates (organic or inorganic) are oxidized, and the electron flow to an electron acceptor provides an energetic pathway for synthesis of biologically relevant energetic molecules. Thus it is not surprising that a wide array of different electron acceptors have been "discovered" by the microbial world, including solid metal oxides, some of which have redox potentials that would qualify them as excellent electron acceptors. However, these metals also offer mechanistic challenges to the microbes when it comes to electron exchange reactions: 1) can bacteria sense and move towards insoluble electron acceptors, and if so, how do they do it; and, 2) what mechanisms are employed for the extracellular transfer of electrons between their cytochromes and the solid metal oxides? With regard to the first question, it is clear from studies with metal oxides, as well as with redox-poised electrodes, that microbes in the group *Shewanella* are capable of sensing and responding to redox potentials. What is not clear is the mechanism involved in this sensing. Several specific mutants have been characterized some of which completely abolish the ability to sense the insoluble redox environment, but at the time of this writing, no consensus with regard to the mechanism(s) of either sensing or response can be specified. With regard to electron transfer, it is clear that a number of outer membrane proteins are key to extracellular electron transport: of noted importance are also cell motility and movement, biofilm formation, and the interaction of electron shuttles and bacterial nanowires. In the spirit of Terry Beveridge, these issues will be discussed, with a focus on methods often used by Terry, including imaging, biochemistry, biophysics, and logic.

In search of the microbe/solid interface: A new approach using super-resolution vertical scanning interferometry measurements

K.H. NEALSON^{1*}, M.S. WATERS¹, M.Y. EL-NAGGAR¹,
C. FISCHER², R.S. ARVIDSON² AND A. LUTTGE²

¹University of Southern California, Los Angeles, CA
(*correspondence: KNealson@jcvl.org)

²Rice University, Houston, TX 77005

The analysis of initial bacterial attachment to solid surfaces is crucial for an improved and quantitative understanding of the development of biofilms on surfaces. Biofilms on rock, metal and glass surfaces play key roles in natural and engineered systems, in diverse processes ranging from weathering and corrosion to charge transfer in microbial fuel cells. Here we present the results of a study using *Shewanella oneidensis* MR-1 as a model organism. We used Vertical Scanning Interferometry (VSI) and Atomic Force Microscopy (AFM) to investigate the initial stages of cell attachment to glass, steel, aluminum, and carbonate surfaces. Although VSI results obtained using opaque and translucent surfaces are unambiguous, highly-reflective metal surfaces such as polished steel occasionally produce apparent observational artifacts. In these cases, bacteria appear as rod-shaped pits rather than as "positive" cells on the steel surface. This inversion is corrected when the bacteria are treated to increase their opacity. This phenomenon is the result of an interaction between light white light reflected from the bacteria's top membrane surface, and the light reflected from the bacteria-metal interface. These results suggest that (1) information can be recorded from the bacterial cell membrane and bacteria on surfaces using VSI; (2) in addition, with appropriate modifications to the analytical software, these data may offer a unique window for direct study of the bacterial/substrate interface. This optical information, a superposition of at least two correlograms, can thus be used for quantitative observations. In concert with recent progress of super-resolution techniques, imaging and characterization of the previously invisible bacteria-substrate interface *in vivo* will provide new insights into interactions that occur at this important junction.

The impacts of Sn-W, Ba-Pb-Zn and W-Au-Sb old mine workings on the environment at central Portugal

A.M.R. NEIVA¹, I.M.H.R. ANTUNES²,
P.C.S. CARVALHO¹ AND M.M.V.G. SILVA¹

¹Department of Earth Sciences, University of Coimbra,
Portugal (neiva@dct.uc.pt)

²Polytechnic Institute of Castelo Branco, Portugal

At Segura, granitic pegmatite veins with cassiterite and lepidolite, hydrothermal Sn-W quartz veins and Ba-Pb-Zn quartz veins intruded the Cambrian schist-metagraywacke complex and Variscan granites. They were exploited for Sn, W, Ba and Pb until 1953. At Sarzedas, W-Au-Sb quartz veins and Sb-Au felsitic dikes intersect the complex and were exploited for W, Au and Sb until 1951. Tin, W, B, As and Cu anomalies in soils and stream sediments from Segura are related to Sn-W quartz veins, whereas Ba, Pb and Zn anomalies in soils and stream sediments from this area are associated with Ba-Pb-Zn quartz veins. At Sarzedas, Sn, W, As and Sb anomalies in soils and W, Pb and Sb anomalies in stream sediments are associated with W-Au-Sb quartz veins and Sb-Au felsitic dikes. The contents of trace elements decrease from soils to stream sediments and waters, due to their relatively low mobility. Soils from Sarzedas must not be used for agriculture, human residence, commerce and industry due to their high Sn, As and Sb contents, whereas soils from Segura should not be used for agriculture and human residence due to their high Sn, B, As and Ba contents and industry due to the high As content. Among these trace elements, the most abundant in soils and stream sediments are Sb at Sarzedas and Ba at Segura. There is no significant acid drainage associated with old mine workings in both areas due to neutralization of acid waters, attributed to marble intercalations in the schist-metagraywacke complex and also siderite in the mineralized veins and dikes from Sarzedas. At Segura, waters associated with Sn-W quartz veins and As anomalies in soils are the richest in As, whereas the waters related to the Ba-Pb-Zn quartz veins are the richest in Fe and Mn. These waters from Segura should not be used for human consumption and agriculture due to their high As, Fe and Mn contents, whereas waters related to W-Au-Sb quartz veins and Sb-Au felsitic dikes from Sarzedas must not be used for human consumption due to their high Fe, Mn and Sb contents. Arsenic, Fe and Mn reach higher contents in waters from Segura than in those from Sarzedas. The W-Au-Sb and Sb-Au old mine workings caused higher impacts on soils and stream sediments, but lower impacts on waters than Sn-W and Ba-Pb-Zn old mine activities.

Sr, Nd, Pb and Hf evidence for two-plume mixing beneath the East African Rift System

W.R. NELSON^{1*}, T. FURMAN¹ AND B. HANAN²

¹Pennsylvania State Univ., University Park, PA 16802

(*correspondence: wnelson@geosc.psu.edu)

(furman@geosc.psu.edu)

²San Diego State University, San Diego, CA 92182

The complexities of the East African Rift System revolve around two areas of mantle upwelling presently located beneath Afar (NE Ethiopia) and the Tanzania craton and their interaction with the overlying lithosphere. Over the past 40 million years, the thermal upwellings or plumes produced chemically distinct lavas in NE Ethiopia and Turkana (N Kenya) respectively, implying separate source regions. Prior to this study, there was no compelling evidence indicating any interaction between the two plumes. However, new Sr, Nd, Pb, and Hf isotopic data from three areas on the eastern Ethiopian plateau between Turkana and Afar suggesting the HIMU-like Turkana source contributed to 24-26 Ma magmatism in central Ethiopia, and its influence decreased from southwest to northeast Ethiopia. [1]

The origin and relationship between the two plumes are not straight forward. Based on its eruptive style and high ³He/⁴He ratios ($R/R_a \leq 19$) the Afar plume likely originated as a classic deep-mantle thermal plume. [2] The HIMU signature manifest in 40-26 Ma Turkana lavas and 26-23 Ma Ethiopian lavas could be derived from either deep mantle recycling of oceanic crust or lithospheric melting. However, the presence of high-Ni olivine in both HIMU-like lavas in Turkana and Ethiopia suggest derivation from a pyroxenite source (recycled oceanic crust) instead of mantle peridotite. [3, 4] Lavas unequivocally associated with Afar do not contain high-Ni olivine. [5].

There are two plausible explanations for the mixing trends recorded in Ethiopian lavas: (1) the Turkana source experienced northward flow between 23 and 26 Ma, mixing with the Afar plume to produce the observed geochemical signatures, or (2) the Afar plume is more heterogeneous than previously recognized, and the trends are mixtures of those heterogeneities. Spatial and temporal geochemical data appear to support the northward flow model.

[1] Furman *et al.* (2006) *J Petrol* **47**, 1221-1244. [2] Pik *et al.* (2005) *Chem. Geol.* **226**, 100-114. [3] Sobolev *et al.* (2005) *Nature* **434**, 590-697. [4] Locke *et al.* (2008) *GCA*, this volume. [5] Rooney *et al.* (2007) *J Geophys Res.* **112**, B10201, doi,10.1029/2006JB004916.

Refining sources and sinks in the global Molybdenum cycle

N. NEUBERT^{1*}, A. R. HERI¹, T.F. NÄGLER¹,
M.E. BÖTTCHER² AND I.M. VILLA¹

¹Institut für Geologie, Universität Bern, Switzerland

(*correspondence: neubert@geo.unibe.ch)

²Leibnitz Institut für Ostseeforschung, Warnemünde, Germany

(michael.boettcher@io-warnemuende.de)

Molybdenum (Mo) is the most abundant trace metal in the ocean and plays an important role in the nitrogen metabolism of planktonic organisms. Recently Mo isotope fractionation became more and more important as a new proxy for the oxygenation history of the oceans and atmosphere. In this context, it is important to establish the sinks and sources of the oceanic Mo cycle. In oxygenic water Mo exists as the molybdate MoO_4^{2-} . Mean Ocean Molybdenum (MOMO) has a concentration of 105nM and a heavy isotopic composition of $\delta^{98/95}\text{Mo} = 2.3\text{‰}$ relative to our standard [1].

The Black Sea is the archetype sink for anoxic and euxinic sedimentation. A detailed profile from the NW shelf to the deep Black Sea shows that Mo removal into surface sediments is related to the amount of free $\text{H}_2\text{S}_{\text{aq}}$. Complete fixation requires a critical $\text{H}_2\text{S}_{\text{aq}}$ concentration ($>11\mu\text{M}$, [2]). Below this concentration, unreactive molybdate coexist with thiomolybdate, which causes isotope fractionation between sediments and bottom water.

Regarding Mo sources, the average Mo river influx to the oceans is less well established. Based on silicate rocks [1] and molybdenites [3] the Mo isotopic composition is assumed to be between -0.4 and +0.6‰. Our river results show variable $\delta^{98/95}\text{Mo}$, between 0 and 1.8‰. The range is similar to [4]; however, the variations we observe in both, $\delta^{98/95}\text{Mo}$ and Mo concentration, clearly indicate that several different processes are operating, suggesting that the modelling of [4] significantly underestimates the complexities of the riverine Mo system and thus global continental runoff. Further, in view of the heavy industrial use of Mo, it is essential to exclude anthropogenic effects to discriminate natural and anthropogenic Mo.

[1] Siebert *et al.* (2003) *EPSL* **211**, 159-171. [2] Erickson & Helz (2000) *GCA* **64**, 1149-1158. [3] Barling *et al.* (2001) *EPSL* **193**, 447-457. [4] Archer & Vance (2007) *GCA* **71**, 15, Suppl., A47.

Molybdenum concentrations in chondrites, stony and iron meteorites

E.M. NEUHEIMER^{1*}, M.E. WIESER¹ AND
J.R. DE LAETER²

¹Department of Physics and Astronomy, University of
Calgary, Canada (mwieser@phas.ucalgary.ca)
(*correspondence: emneuhei@ucalgary.ca)

²Department of Applied Physics, Curtin University of
Technology, Western Australia
(J.DeLaeter@curtin.edu.au)

Variations in isotopic amount ratios and elemental concentrations among meteorite classes has been researched intensely and well documented. Isotopic abundances, including variations due to fractionation, as well as elemental concentration of molybdenum is of particular interest in regards to meteorites. Enrichment in one isotope compared to another can indicate nucleosynthetic sources and the nucleosynthetic stage at which formation occurred. The main distinguishing factor for meteorite classification is iron content. Molybdenum is moderately siderophile which indicates that variation in molybdenum concentration amongst meteorite classes is expected. Carbonaceous chondrites represent the primordial material from which our solar system formed. Subsequent differentiation of Mo in planetesimals results in Mo concentration variations in stony and iron meteorites.

Nineteen meteorites were prepared chemically for analysis under strict conditions to eliminate possible contamination, in particular, Zr and Ru isobaric interferences. The selection of meteorites includes rare carbonaceous chondrites such as Tagish Lake, Allende and Murchison. Each sample was analysed for Mo concentration using a double spike technique by thermal ionization mass spectrometry. The Mo concentration of chondritic samples varied from 1 - 2.5 ppm while iron meteorites ranged from 1 – 29 ppm. Zagami and a particular sample of Sayh al Uhaymir had concentrations of ~0.5 ppm. These concentrations are in accordance with Mo concentrations measured in: Orgueil, Ivuna and Mundrabilla [1].

[1] Wieser & DeLaeter (2000) *Fresenius J. Anal Chem.* **368**, 303-306.

Ultra-depleted domains in the oceanic mantle lithosphere

ELSE-R. NEUMANN AND NINA S.C. SIMON

Department of Geosciences, University of Oslo, P.O. Box
1047 Blindern, NO-0316 Oslo, Norway
(e.r.neumann@geo.uio.no, n.s.c.simon@fys.uio.no)

Many mantle xenoliths sampled in ocean islands (OI) are ultra-refractory spinel harzburgites (OIu: high $cr\#_{sp}$, high Fo_{ol} , low $(Al_2O_3)_{opx}$, low HREE in opx) that, on average, are more refractory than MOR peridotites (MORP). OIu are common in the Canary Islands, Madeira, Cape Verde Kerguelen, Samoa and Loihi seamount. OIu rocks formed by high degrees of partial melting leading to total exhaustion of primary cpx. minor amounts of secondary cpx has formed by unmixing from opx and recrystallization. High Re-Os model ages indicate that some OIu rocks are significantly older than the surrounding oceanic crust, and thus cannot represent mantle residues complimentary to this crust. Laser analyses of cpx in some OIu xenoliths from the Canary Islands give $^{87}Sr/^{86}Sr$ ratios of 0.7027-0.7028, i.e. well below those of Canary Islands basalts. This implies that the ultra-refractory nature of the Canarian OIu was acquired some time in the past. Thus they do not represent plume material, and have not acquired their ultra-refractory nature through recent, plume-related processes. We interpret the OIu xenoliths as fragments of "exotic" material (continental mantle or recycled oceanic mantle lithosphere) trapped in the oceanic mantle lithosphere. Strong similarities (in whole rock and mineral major element compositions) to some series of oceanic sub-arc mantle suggest that the OIu peridotites may have acquired their ultra-refractory nature through similar processes (fluid-fluxed melting). The proportion of ultra-refractory peridotites among ocean island xenoliths is high; of 241 OI harzburgites and lherzolites 68% have Fo contents ≥ 90.5 , i.e. as high or higher than in average MORP. Their common presence in ocean islands, and their presence along some mid-ocean ridges and in sub-arc mantle, suggests that ultra-refractory material may be important in the convecting mantle.

Structure of silicate melts using *in situ* high temperature X-ray absorption on light elements (Mg, Si, Al, K, Ca)

DANIEL R. NEUVILLE¹, DOMINIQUE DE LIGNY²,
LAURENT CORMIER³, ANNE-MARIE FLANK⁴ AND
PIERRE LAGARDE⁴

¹Physique des Minéraux et Magmas, IPGP, CNRS, 4 place Jussieu, 75005 Paris, France

²LPCML, UCBL, 12 rue Ampère, 69622, Villeurbanne, France

³IMPMC, Universités Paris 6 et 7, CNRS UMR 7590, 140 rue de Lourmel, 75015 Paris France

⁴SOLEIL-CNRS-PSI, Swiss Light Source, CH-5232 Villigen – PSI

Structure of silicate and aluminosilicate melts is not well known at high temperature. X-ray absorption spectroscopy is a very specific and interesting way to probe the network structure and more specifically the Al and Si surrounding.

Recent developments on X-ray absorption spectroscopy at light K-edges, made on the LUCIA beamline at the Swiss Light Source, enable to measured XANES spectra at high temperature on the Mg, Al, Si, Al, K and Ca K-edges. We have investigated crystal and melts from room temperature up to the liquidus.

All these observations on the XANES on the K-edge of light elements are correlated with simulations using FDMNES.

Origin of non-linear mass dependent fractionation in Nd

K. NEWMAN^{1*}, P.A. FREEDMAN¹, J. WILLIAMS¹ AND
N. S. BELSHAW²

¹Nu Instruments Ltd, Unit 74, Wrexham Industrial Estate, LL13 9XS, UK (*correspondence: karla@nu-ins.com)

²Dept. of Earth Sciences, Univ. of Oxford, OX1 3PR, UK

Investigations of experimental skimmer cones revealed significant non-linear mass dependent fractionation in the measured Nd isotope ratios. It is proposed that the origin of this non-linear mass bias is the formation of NdO⁺ at (or very close to) the skimmer surface. The degree of oxide formation, and hence fractionation, is isotope dependent but is not a linear function of mass (Fig. 1).

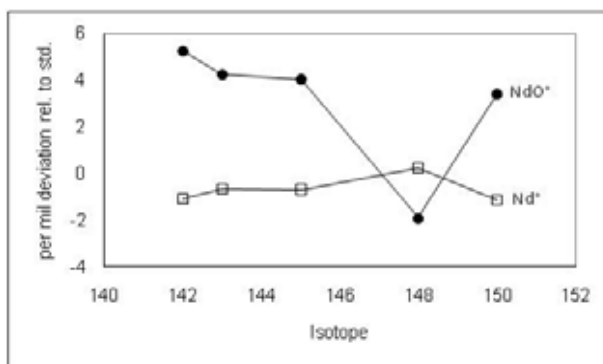


Figure 1: Normalised to $^{146}\text{Nd}/^{144}\text{Nd} = 0.7219$ (error bars are smaller than the data points).

A decrease in the $^{x}\text{Nd}/^{144}\text{Nd}$ ratio, relative to standard values, in Nd⁺ is associated with a concomitant increase in the same ratio in NdO⁺ (and vice versa). The correlation between the metal and oxide species is consistent with mass balance calculations. The magnitude of this effect was dependent on conditions at the skimmer surface (geometry, surface coating, etc.) and could be suppressed by the addition of small amounts of N₂ to the carrier gas flow.

The non-linear fractionation observed is shown to correlate with deviations (from a linear function of mass) in the nuclear charge radii.

A simple energy-resonant ion-atom reaction is postulated to explain these observations. The other REEs and their oxide formation will be discussed.

Non-linear mass fractionation effects were not observed in commercially released Nu skimmers. However, non-linear contributions to the mass bias may be present in any system at very low levels (particularly in the absence of air leaks in the inlet) and could be a source of analytical uncertainty.

The marine sulfate-oxygen isotope record of the early Toarcian anoxic event

R.J. NEWTON, N. KAFOUSIA, E. REEVES, P.B. WIGNALL AND S.H. BOTTRELL

Earth & Biosphere Institute, School of Earth & Environment, University of Leeds, Leeds, LS2 9JT, UK

Here we present two records of marine $\text{SO}_4\text{-O}$ isotopes derived from carbonate associated sulfate (CAS) across the Toarcian anoxic event, one from a Tethyan open ocean margin (Tibet) and the other from within the European Epicontinental Sea (EES, Yorkshire, UK). Limestones from Tibet record average $\text{SO}_4\text{-}\delta^{18}\text{O}$ of $+13.1\pm 1.3\text{‰}$ across the interval with no systematic change. Belemnites from Yorkshire however record considerably heavier values which change in a systematic way. These start at $\sim +15\text{‰}$ in the uppermost Pliensbachian and rapidly climb to $+19\text{‰}$ across from the *paltum* to *clevelandicum* ammonite subzones in the lowermost Toarcian. A $\text{SO}_4\text{-}\delta^{18}\text{O}$ value of $+19\text{‰}$ is then maintained until the top of the *exaratum* subzone (which also marks the end of the Toarcian OAE in the EES), whereupon a slow but variable decline begins back to $\sim +15\text{‰}$ in the *levesqui* subzone.

These differences are paralleled by changes in the $\text{SO}_4\text{-}\delta^{34}\text{S}$ isotope composition in the two sections with Tibet showing little change (mean $+19.1\pm 1.8\text{‰}$) and Yorkshire exhibiting a large positive excursion ($+17$ to $+23\text{‰}$). This excursion does not begin until the basal *exaratum* subzone, 4 subzones after that in $\text{SO}_4\text{-O}$. The differences in S isotope composition between the two sections provide evidence of the isolation of the EES from the global ocean.

The isotopic composition of $\text{SO}_4\text{-O}$ in marine waters reflects the cycling of S between reduced and oxidised states, rather than the simpler balance of inputs and outputs that control the sulfate-sulfur isotope signal. This shortens the residence time of sulfate in marine waters by at least an order of magnitude – a feature apparent in the lag between these excursions. The change to heavier values in predominantly oxic sediments is more problematic to explain. Two potential mechanisms are suggested; the first involves the development of a gradient in dissolved oxygen isotopes, and the second an increase in intermediate S species driven by increased sulfate reduction and reoxidation. Both of these would have to be driven by increased productivity and oxidation of organic matter. If this interpretation is correct the EES $\text{SO}_4\text{-O}$ data must therefore record the change in conditions (nutrient availability?) that ultimately lead to the Toarcian anoxic event in the EES.

Thermodynamics of $\text{SiO}_2\text{-H}_2\text{O}$ at the second critical end point

R.C. NEWTON AND C.E. MANNING*

Dept. of Earth and Space Sciences, Univ. California, Los Angeles, CA 90095, USA

(*correspondence: manning@ess.ucla.edu)

At >8 kbar, quartz solubility in the vapor phase increases sharply along the H_2O -saturated melting curve, and projected compositions of liquid and vapor become coincident at a proposed critical end point near 10 kbar and 1080°C [1]. To constrain thermodynamic properties and speciation near the possible end point, we measured quartz solubility in H_2O at 10 kbar and $700\text{--}1130^\circ\text{C}$, extending results of earlier work [2]. Results confirm that the compositional dependence on temperature possesses a vertical tangent near 1080°C , as required at a critical point. The critical fluid is a nearly equimolar mixture of SiO_2 and H_2O . The SiO_2 activity (a_{SiO_2}) in near-critical quartz-saturated $\text{SiO}_2\text{-H}_2\text{O}$ fluids, determined from depression of the melting point of quartz, is nearly constant at 0.65 at SiO_2 mole fraction (X_{SiO_2}) of 0.2 to 0.6. Corresponding H_2O activities are surprisingly high ($a_{\text{H}_2\text{O}}\approx 0.93$) in the same composition range. The thermodynamics of quartz dissolution is defined by the reaction $\text{SiO}_2(\text{q}) + n \text{H}_2\text{O} = \text{Si}(\text{OH})_4 \cdot \text{H}_2\text{O}_{(n-2)}$, where n is the hydration number of the monomeric reference solute and $n-2$ is the number of hydrogen-bonded H_2O molecules. Newton and Manning [3] measured quartz solubility in $\text{NaCl-H}_2\text{O}$ and $\text{CO}_2\text{-H}_2\text{O}$ fluids at high P and T . New data was collected in the latter system as part of the present study. A Walther-Orville [4] plot of $\log a_{\text{SiO}_2}$ activity (determined from polymerization theory [5]), versus $\log a_{\text{H}_2\text{O}}$ (from measurements in the two fluid subsystems [6, 7]) at 800°C and 10 kbar shows that $n=2$ for $\text{NaCl-H}_2\text{O}$; that is, that hydrogen bonded H_2O is negligible in the ionic salt system. In quartz-saturated $\text{CO}_2\text{-H}_2\text{O}$ fluids, however, n varies from 4 at high $a_{\text{H}_2\text{O}}$ to 2 at low $a_{\text{H}_2\text{O}}$. We infer from these findings that hydrogen bonding to polymeric silica clusters explains both the high H_2O activity of near-critical $\text{SiO}_2\text{-H}_2\text{O}$ fluids and the monotonous melting point of quartz, independent of melt composition, as a result of high H_2O activity in the melts.

- [1] Kennedy *et al.* (1962) *AJS* **260**, 501–521. [2] Manning (1994) *GCA* **58**, 4831–4839. Newton & Manning (2000) *GCA* **64**, 2993–3005. [3] Walther & Orville (1983) *Am. Min.* **68**, 731–741. [4] Newton & Manning (2003) *CMP* **146**, 135–143. [5] Aranovich & Newton (1996) *CMP* **125**, 200–212. [6] Aranovich & Newton (1999) *Am. Min.* **84**, 1319–1332.

The role of exopolymers in the speciation of redox-sensitive metals: Implications for metal cycling in biofilms

BRYNE T. NGWENYA

School of GeoSciences, University of Edinburgh, Grant Institute, West Mains Road, Edinburgh EH9 3JW, UK
(bryne.ngwenya@ed.ac.uk)

We are studying the kinetics of Cr(VI) and Fe(III) reduction using EPS and non-EPS producing mutants of *Pseudomonas putida* in order to quantify the role of biofilms in the cycling and speciation of redox-sensitive metals. Our justification is that in some natural environments (e.g. subsurface), respiration is limited by lack of labile organic matter, requiring indigenous bacteria to find alternatives sources. Since bacteria form biofilms in nature, we hypothesized that EPS represents a labile pool of dissolved organic matter¹, because > 90% of the biomass in biofilms is in the form of EPS².

Our study involves two complimentary approaches. We conduct metal reduction experiments using planktonic cells, with metal speciation analysis using traditional wet chemical methods (diphenylcarbazide for hexavalent chromium and ferrozine for ferrous iron). Additionally, we perform metal reduction experiments using biofilms grown on glass slides, and determine metal speciation by XPS.

Preliminary results using Cr(VI) in planktonic cultures show that the reduction rate follows first order kinetics with respect to Cr(VI) concentration, consistent with previous studies. Moreover, a higher reduction rate is observed in the presence of EPS, and this appears to scale with the dissolved organic carbon in the suspensions. These findings imply an important role for EPS in maintaining viable microbial populations through recycling of both metals and organic matter.

[1] Tournay *et al.* (2008) *Chem. Geol.* **247**, 1-15. [2] Liu *et al.* (2007) *J. Photochem. Photobiol. A, Chem.* **190**, 94-100.

Low mature coal-derived gases from the Turpan-Hami Basin, Northwest China

YUNYAN NI, JINXING DAI, QINGHUA ZHOU, ANPING HU
AND CHUN YANG

Research Institute of Petroleum Exploration and Development, PetroChina, Beijing 100083, China
(niyy@petrochina.com.cn)

Natural gas can be formed from microbial activities on sedimentary organic matter (biogenic gas, nearly exclusively composed of CH₄) and from the thermal breakdown of organic matter (thermogenic gas, composed of CH₄ and higher homologues). According to the source rock type, thermogenic gas can be further subdivided into coal-derived gas (terrestrial) and oil-type gas (marine). Since natural gases are dominated by some simple and low-molecular hydrocarbons, stable carbon isotopic values have great importance on genetic information. Here we show some low mature coal-derived gas with significantly low carbon isotopic values of methane from the Turpan-Hami Basin, Northwest China.

The Turpan-Hami Basin is located in the eastern Xinjiang, Northwest China and has an area of 53500 km². The main reservoir rocks for natural gases in the basin are Jurassic coal measures and the source rocks are dominated by middle-late Jurassic coal measures. Hydrocarbon gases account for more than 97% of the natural gases from Turpan-Hami Basin, and the content of non-hydrocarbon gases (N₂, CO₂, etc.) is quite low, averagely less than 2%. C₁/C₁₋₅ ratios are normally less than 0.9. Carbon isotopes demonstrate an orderly isotopic trend ($\delta^{13}\text{C}_1 > \delta^{13}\text{C}_2 > \delta^{13}\text{C}_3 > \delta^{13}\text{C}_4$). For C₁, C₂, C₃ and C₄, the carbon isotopic ratios are averaged at -42.2‰, -26.7‰, -25.6‰ and -24.8‰, respectively.

Compared to oil-type gases, coal-derived gases are isotopically heavier (-22‰~-38‰ for $\delta^{13}\text{C}_1$) and drier (more methane-rich) (Patience, 2003). The relatively low $\delta^{13}\text{C}$ values and content of methane in the Turpan-Hami Basin is due to the fact the these natural gases are normally from the coal-derived oil and gas fields in the Taibei depression where the middle-late Jurassic coal measures have very low maturity level (Ro of 0.5%-0.9%). Mixing from biogenic gases can be excluded since no evidence of the presence of biogenic gases in this basin has ever been reported. It is concluded that coal-derived gases can be formed under conditions of very low temperature and low level of maturity.

[1] Patience, R.L. (2003) Where did all the coal gas go? *Org. Geochem.* **34**, 375-387.

Redox dynamics of mixed metal (Mn, Cr, and Fe) ultrafine particles

PETER S. NICO^{1*}, BENJAMIN M. KUMFER²,
IAN M. KENNEDY² AND CORT ANASTASIO³

¹Earth Sciences Division, Lawrence Berkeley National Laboratory, One Cyclotron Rd., Berkeley, CA 94720, USA (*correspondence: psnico@lbl.gov)

²Department of Mechanical and Aeronautical Engineering, University of California, Davis, CA 95616

³Department of Land, Air & Water Resources, University of California, Davis, CA 95616

Recent epidemiological studies have demonstrated a correlation between exposure to fine particulate matter and an increased incidence of cardiovascular morbidity and mortality. Unfortunately the mechanisms behind this correlation remain largely unknown. Ultrafine particles (smaller than 100 nm) have been reported to be particularly relevant pathologically due to their small size and high reactivity. The primary constituents of ambient ultrafine particles are carbon, organic compounds and metals. The metals, in particular the transition metals, may play a key role in determining the toxicity of ultrafine particles. Of the transition metals, Fe, Cr, and Mn are of particular interest because of their abundance and the fact that their redox chemistry alters their bioavailability and toxicity.

The impact of particle composition on metal oxidation state, and on changes in oxidation state with simulated atmospheric aging, are investigated experimentally in flame-generated nanoparticles containing Mn, Cr, and Fe. The results demonstrate that the initial fraction of Cr(VI) within the particles decreases with increasing total metal concentration in the flame. In contrast, the initial Mn oxidation state was only partly controlled by metal loading, suggesting the importance of other factors. Two reaction pathways, one reductive and one oxidative, were found to be operating simultaneously during simulated atmospheric aging. The oxidative pathway depended upon the presence of simulated sunlight and O₃, whereas the reductive pathway occurred in the presence of simulated sunlight alone. The reductive pathway appears to be rapid but transient, allowing the oxidative pathway to dominate with longer aging times, i.e. greater than ~8 hours. The presence of Mn within the particles enhanced the importance of the oxidative pathway, leading to more net Cr oxidation during aging implying that Mn can mediate oxidation by removal of electrons from other particulate metals.

Investigation of Thallium isotope fractionation during sorption to Mn oxides

SUNE G. NIELSEN¹, CAROLINE L. PEACOCK² AND
ALEX N. HALLIDAY¹

¹Dept. of Earth Science, University of Oxford, Parks Rd, OX1 3PR, UK

²National Oceanography Centre Southampton, University of Southampton, Waterfront Campus, European Way, Southampton SO14 3ZH, UK

Thallium (Tl) is one of the heaviest elements for which variation in natural stable isotope composition has been recorded. To date, the largest isotope fractionation factor reported has a magnitude of about 20 ε²⁰⁵Tl-units (where ε²⁰⁵Tl = 10⁴ × ((²⁰⁵Tl/²⁰³Tl)_{sample} - ²⁰⁵Tl/²⁰³Tl_{NIST 997}) / (²⁰⁵Tl/²⁰³Tl_{NIST 997})) and occurs between seawater and hydrogenetic marine ferromanganese (FeMn) crusts [1]. Recently, it was proposed that Tl isotope variations of this size most likely occur during equilibration of the two valence states of Tl, +1 and +3 [2].

Mn oxide phases are extremely efficient scavengers of dissolved trace-metals. Tl is highly enriched in marine FeMn deposits relative to seawater and empirical studies show positive Tl-Mn correlations [3]. A previous x-ray absorption spectroscopy (XAS) study of Tl sorption by the principle Tl-carrier in Fe-Mn crusts, δ-MnO₂, suggests that Tl is almost exclusively present in this mineral as Tl³⁺, despite the solution used for sorbing Tl onto δ-MnO₂ consisted solely of Tl⁺ [4]. Hence, we hypothesize that Tl isotopes might fractionate as a function of Tl oxidation by different Mn oxide phases.

Here we have performed Tl-sorption experiments at seawater pH with δ-MnO₂ (7Å-vernadite), 10Å-vernadite and todorokite, equilibrated over various time scales. Tl-sorbed Mn oxides were investigated with XAS for Tl oxidation state and Tl crystal-chemistry. Aliquots of the same Tl-sorbed samples were separated for Tl isotope composition determination. Supernatants were also kept for Tl isotope analysis.

Thallium speciation and isotope compositions for the Tl-sorbed Mn Oxides will be presented and discussed in the context of theoretical predictions. Additionally, we will present Tl XAS analyses of a range of natural FeMn crust samples, for which Tl isotope data is already available [1].

[1] Rehkämper *et al.* (2002) *EPSL*. [2] Schauble (2007) *GCA*. [3] Li (1982) *GCA*. [4] Bidoglio *et al.* (1993) *GCA*.

Stable isotope systematics of coalbed methane: Desorption and production

MARTIN NIEMANN^{1*} AND MICHAEL J. WHITICAR²

¹Geoservices S.A., 93151 Le Blanc Mesnil, France

(*correspondence: martin.niemann@geoservices.com)

²School of Earth and Ocean Sciences, University of Victoria,
V8W 2Y2, Victoria, BC, Canada (whiticar@uvic.ca)

Coalbed methane (CBM) is a growing resource for natural gas. Although there has been considerable basic geochemical research on CBM, the application of stable carbon and hydrogen isotope ratios of CBM are not common.

In our study, 1000 CBM samples were collected and analyzed by CF-IRMS during 10 different sample campaigns in 7 different coal bearing basins. Seven sample sets were collected during desorption experiments and 3 were collected from CBM production wells. The coals range in maturity from subbituminous A to anthracite and cover a wide range of different maceral compositions. Samples span canister desorption times of up to 2773 hours and production time of up to 6312 hours.

Gas compositions do not show any significant trends with increasing production/desorption time, however, the $\delta^{13}\text{C}-\text{CH}_4$ values do vary with production/desorption time. Samples from desorption experiments express the expected ^{13}C enrichment for CH_4 with increasing desorption time (isotope shifts up to 43.4‰). In specific instances, a ^{12}C enrichment is also observed (isotope shifts up to 3.1‰). Production samples show a trend opposite to the desorption samples, with a general depletion in ^{13}C with increasing production time (isotope shifts up to 35.8‰).

$\delta^{13}\text{C}-\text{CH}_4$ values do not display the expected compositions of CH_4 generated from coals. This indicates the influence of secondary processes. The processes mixing, adsorption, desorption and diffusion are significant for the alteration and liberation of CBM. The significant alteration of the CBM gases is treated as a combined effect of these processes, due to the challenges in reliably differentiating these processes.

A mixing model is presented to explain unexpected $\delta^{13}\text{C}-\text{CH}_4$ trends observed for some production samples. Interactions of mixing, desorption and diffusion as a function of time and distance is presented as a reasonable explanation for the observed trends.

Obsidian provenance studies from the Chalcolithic Sites of the Eastern Lake Urmia, Northwestern Iran

KAMAL ALDIN NIKNAMI AND
AHMAD CHAYCHI AMIRKHIZ

Department of Archaeology, University of Tehran, Enghlab
Street, Tehran, Iran (kniknami@ut.ac.ir,
ahmadchaychi@yahoo.com)

In 2005-2006 a major archaeological survey of obsidian finding and characterization was conducted to study the long-term use of obsidian in the eastern shores of Lake Urmia region, Northwestern Iran. In Iran, the early works suggested that almost all archaeological obsidians came from the Nemrud Dağ sources somewhere around the Lake Van in Asia Minor (Turkey). Through a characterization procedure it appeared that samples presenting the elemental composition might present similarities which can be attributable for a nearby unknown source in the region. This means that these samples had to come from yet unknown but possibly not very distant sources. Such compositional similarities between artifacts and sources material (geological samples) were found for the region where a large part of the raw obsidians could however be sourced. In order to improve our knowledge of Iranian obsidians and eventually refine provenance criteria we revisited about 56 Chalcolithic sites and some source areas. Both obsidian sources and samples compositions then were determined by PIXE and EDXRF instruments. This paper presents our first set of results from the trace elemental analysis of both source and worked obsidians that have provided important new data concerning the diachronic relationship between lithic technology and raw material in the northwestern Iran.

An empirical method for estimating instream pre-mining pH and dissolved Cu concentration in catchments with acidic drainage and ferricrete

DAVID A. NIMICK^{1*}, JOSEPH T. GURRIERI² AND GEORGE FURNISS³

¹U.S. Geological Survey, Helena, MT 59601, USA
(*correspondence: dnmick@usgs.gov)

²USDA-Forest Service, Ogden, UT 84401, USA
(jgurrieri@fs.fed.us)

³Department of Geology, University of Montana, Missoula, MT 59812, USA (comogeo@gmail.com)

An empirical method is proposed for assessing background water quality of streams affected by historical mining. Stream-specific equations were generated from relations between either pH or dissolved Cu concentration in stream water and the Fe/Cu concentration ratios in Fe-precipitates presently forming in three acidic streams in Montana, USA. The equations and Fe/Cu ratios for pre-mining deposits of alluvial ferricrete along each stream then were used to reconstruct estimated longitudinal profiles of pre-mining pH and dissolved Cu concentration. The method assumes that alluvial ferricretes and modern Fe-precipitates share a common origin and that the Cu content of Fe-precipitates remains constant during and after conversion to ferricrete. The method was evaluated by applying it in a fourth, naturally acidic stream unaffected by mining, where estimated pre-mining pH and Cu concentrations were similar to present-day values and by demonstrating that inflows from unmined areas had consistent effects on both the pre-mining and measured profiles of pH and Cu concentration. Using this method, it was estimated that mining has affected about 0.5 m of Daisy Creek, 1.8 km of Fisher Creek, and at least 1 km of Swift Gulch. Estimated pre-mining pH values were ~0.6 units higher in Daisy Creek, 1-1.5 units higher in Fisher Creek, and 1.3-1.9 units higher in Swift Gulch. Estimated pre-mining dissolved Cu concentrations were almost 40% lower in Daisy Creek and as much as 70% lower in Fisher Creek. Uncertainty in the fate of Cu during this conversion translates to potential errors in pre-mining estimates of as much as 0.25 units for pH and 22% for dissolved Cu concentration.

Planetary differentiation timescales: Insights from physics and chemistry

F. NIMMO*

Dept. Earth & Planetary Sciences, U.C. Santa Cruz, Santa Cruz CA 95064 (*correspondence: fnimmo@es.ucsc.edu)

Introduction

Planetary differentiation involves the delivery of mass and energy, resulting in chemically distinct reservoirs (e.g. crust, core). The formation of these reservoirs provides important geochemical constraints on the timescales and physical processes involved. Here I will discuss two such processes: core formation and magma ocean evolution.

Planetary accretion is rapid: ~1 Myr to build Mars-sized bodies, ~10-100 Myr to finish assembling Earth-sized bodies [1]. Rapidly-formed small bodies are heated primarily by decay of short-lived radioisotopes, which leave behind detectable signatures [2]. Large (Earth-sized) bodies are heated mainly by individual late-stage impacts [3]. Mars-sized bodies are gravitationally heated to an extent determined by the size-spectrum of the impacting bodies [4].

Core Formation

For large bodies, core formation is the result of individual collisions. Depending on the timing of and degree of equilibration during these collisions, measurable ¹⁸²W anomalies will develop [5]. Forward modelling of these processes [6] is hampered by uncertainties in how equilibration and partitioning vary with time [7-8]. Even so, the inferred core formation timescales agree roughly with those predicted from accretion simulations [5, 6].

Less work has been done on core formation of small bodies. Drainage of iron to the core is possible once iron melting begins, and very rapid once silicate melting occurs [9]. Early melting due to radioactive heating should lead to predictable (and testable) correlations between indicators of core formation (e.g. ¹⁸²W or ¹⁰⁷Ag) and of heating (e.g. ²⁶Mg).

Magma Ocean Evolution

Large impacts create regional or global magma oceans [3]. Arguments based on siderophile abundances can only be used to constrain time-averaged magma ocean *P,T* values [10]. Modelling magma ocean duration is complicated because of the uncertain roles of a potentially buoyant crust and/or thick atmosphere. Early Martian isotopic heterogeneities are preserved, suggesting long-lived magma ocean(s) and little convective mixing [11].

- [1] Nagasawa *et al.* (2007) in *Protostars & Planets V*
 [2] Srinivasan *et al.* (1999) *Science* [3] Tonks & Melosh (1993, *JGR*. [4] Senshu *et al.* *JGR* (2002) [5] Kleine *et al.* (2002) *Nature*. [6] Nimmo & Agnor (2006) *EPSL*. [7] Wood *et al.* (2006) *Nature*. [8] Rubie *et al.* (2003) *EPSL*. [9] Stevenson (1990) in *Origin of the Earth*. [10] Righter (2003) *AREPS*. [11] Debaille *et al.* (2007) *Nature*.

Dynamical and thermal implications of Martian core formation timescales

F. NIMMO^{1*} AND C.B. AGNOR²

¹Dept. Earth & Planetary Sciences, U.C. Santa Cruz, Santa Cruz CA 95064 (*correspondence: fnimmo@es.ucsc.edu)

²Astronomy Unit, Queen Mary University of London, London E1 4NS, UK (c.b.agnor@qmul.ac.uk)

The earliest thermal history of Mars depends mainly on the manner in which it accreted. For instance, a Mars built entirely out of small bodies would have been cold and undifferentiated [1]. Conversely, a collision between two bodies each roughly 10% of a Mars mass (M_m) would have been sufficient to initiate global melting [2]. Melting of silicates is important because it allows rapid percolation of iron and thus core formation. The Hf-W isotope system constrains the timing of core formation [3], though the system can also be affected by garnet crystallization.

Estimates of the Martian core formation timescale span a range of ~1-10 Myr [3, 4], primarily because of uncertainties in the bulk mantle Hf/W ratio [5]. Martian accretion may thus have been either relatively rapid or relatively slow. In either case, Mars' formation likely involved collisions with neighbouring protoplanets of comparable mass ("giant" impacts) as well as impacts with much smaller bodies. An impactor hitting Mars generates roughly its own mass in impact melt. Regional magma seas generated by such impacts are one possible explanation for the existence of several ancient and distinct reservoirs on Mars [6].

A Mars which accreted rapidly (~1 Myr) would have melted automatically due to the decay of ²⁶Al, irrespective of the size-spectrum of accreting bodies [2]. On the other hand, a more slowly accreting Mars must have undergone at least one giant impact to ensure melting and differentiation. If the Hf/W data suggest a ~10 Myr core formation timescale, they therefore provide information on the kind of impacts Mars suffered. Further constraints on the accretion history of Mars may be derived by considering its current rather slow spin rate. Accretion involving multiple giant impacts tends to result in planets spinning close to the stability limit (period ~ 3 hrs) [7]. For Mars, a late impactor of mass 0.1 M_m has only a ~3% probability of causing Mars to spin as slowly as it is observed to do. There is thus a relatively narrow window of possible impacts which allow melting and core formation to take place, but do not violate spin constraints.

[1] Senshu *et al.* (2002) *JGR* [2] Rubie *et al.* (2007) *Treatise Geophys.* [3] Kleine *et al.* (2002) *Nature* [4] Jacobsen, (2005) *AREPS* [5] Nimmo & Kleine (2007) *Icarus* [6] Halliday *et al.* (2001) *Space Sci Rev.* [7] Agnor *et al.* (1999) *Icarus*.

Biological controls on the late Archaean atmosphere

EUAN NISBET

Royal Holloway, U. of London (e.nisbet@gl.rhul.ac.uk)

The late Archean atmosphere, like the modern atmosphere, was probably a biological construction. Methanogens may be of great antiquity, as may be anammox planctomycetes. Anoxygenic photosynthesisers may have been present 3.5 Ga ago. Oxygenic photosynthesisers probably appeared about 2.9 Ga ago, at the same time as large scale carbonate reefs [2].

Rubisco specificity may have had a crucial role in atmospheric evolution. Rubisco III in archaeal methanogens has a very high affinity for O₂ and operates in settings with very low molecular oxygen. In contrast, the specificity and compensation controls of Rubisco I in cyanobacteria sustain an atmosphere with O₂ in percent and CO₂ in ppm. These competing enzymes and the greenhouse consequences permit a bistable system, either anoxic or aerobic. Such controls may have worked in tandem with inorganic controls such as the impact of UV shielding on the lifetime of atmospheric oxygen [1].

Atmospheric pressure is today maintained principally by the nitrogen burden. In the late Archaean this may have been subject to the balance between anammox emission of N₂, lightning, and the nitrogen cycle mediated by nitrogenase (which must be protected from oxygen). Collectively, the interaction between specificity of biochemical enzymes and the greenhouse may have shaped the late Archaean biosphere. Inorganic geochemistry would have operated within the wider framework set by the biological controls.

[1] Goldblatt, C., Lenton, T.M., & Watson, A.J. (2006) *Nature* **443**, 683-686. [2] Nisbet, E.G., Grassineau, N.V., Howe, C.J., Abell, P.I., Regelous, M., & Nisbet, R.E.R. (2007) *Geobiology* **5**, 311-335.

Characterization of CL halo in feldspar minerals

H. NISHIDO^{1*}, M. KAYAMA¹, S. TOYODA², K. KOMURO³
AND K. NINAGAWA²

¹Research Institute of Natural Sciences, Okayama University of Science, 1-1 Ridai-cho, Okayama, 700-005, Japan
(*correspondence: nishido@rins.ous.ac.jp)

²Department of Applied Physics, Okayama University of Science, Japan

³Earth Evolution Sciences, University of Tsukuba, Japan

Feldspar occasionally has a visible radiation damage halo surrounding radionuclide-bearing minerals within it. Until now the formation of such halo has not been investigated in detail. In this study, cathodoluminescence (CL) of He⁺ ion implanted feldspar minerals have been measured to characterize the halo for geodosimetry and geochronology.

Single crystals of sanidine (Or₉₀Ab₁₀) and albite (Ab₉₉Or₁) were selected for CL and Raman measurements. He⁺ ion implantation in the sample was performed on a 3M-tandem ion accelerator at 4 MeV corresponding to the energy of alpha-particles from disintegration of ²³⁸U. A CL scanning microscopy (SEM-CL), SEM (JEOL: JSM-5410) combined with a grating monochromator (OXFORD: Mono CL2), was used to measure CL spectra ranging from 300 to 800 nm at 15 kV acceleration voltage and a beam current of 1.0 nA.

CL images of sanidine and albite exhibit CL halo in the surface of He⁺ ion implanted samples. Approximately 15 micro meter width of CL halo might be consistent with theoretical range of alpha-particles from disintegration of ²³⁸U in these feldspar. CL intensity of sanidine gradually decreases from the implantation surface to the inside up to approximately 15 micron meters, over which it jumps up to bulk emission level of non-implanted area. CL line analysis in the section of halo area and Raman spectroscopy reveal that He⁺ implantation causes structural destruction, especially breakage of framework configuration, suggesting reduction of emission centers such as Al-O-Al defect in halo. On the other hand, albite shows the increase of CL intensity exponentially from the surface to the inside, with its maximum at approximately 15 micron meters from the surface. This CL emission from the halo might be assigned to radiation induced luminescence centers formed by He⁺ ion implantation.

C isotopes and multi-elements distribution within individual Proteozoic microfossils

MANABU NISHIZAWA¹, NAOTO TAKAHATA²,
YUJI SANO², YUICHIRO UENO³ AND
SHIGENORI MARUYAMA⁴

¹Department of EPS, Tokyo Institute of Technology, Japan
(nishizawa.m.ac@m.titech.ac.jp)

²Ocean Research Institute, The University of Tokyo, Japan

³Global Edge Institute, Tokyo Institute of Technology, Japan

Early evolution of life during Precambrian time is characterized metabolic development in micro-organisms (e.g. Schopf [1]). Though many of modern micro-organisms share similar cell morphology (e.g. spheroidal, filamentous) they are highly diverse physiologically. Thus, it is inadequate to decipher the physiology of fossil micro-organisms based only on morphology. Carbon isotopes and elemental compositions of individual microfossils have potential to preserve the physiological information such as carbon fixation pathway and substrate [1-3]. We here analyzed carbon isotopes and elemental compositions of individual microfossils from Proteozoic stromatolite, using by NanoSIMS. Using primary Cs⁺ ion beam, carbon isotopes were measured at 1.5 μm spatial resolution, while intracellular distribution of multi elements (H, C, N, P, S) were analyzed at 100 nm spatial resolution. Carbon isotopes and elemental compositions are characteristic to fossil cell morphology (filamentous and radial shape). However, within the microfossils with similar morphology, significant variations in carbon isotopes (20‰) and elemental compositions are also observed. Based on the carbon isotopes and elemental compositions as well as information on morphology and petrography, we will discuss the physiology of those microfossils.

[1] Schopf (1994) in Bengtson (ed.) *Early Life on Earth*, Columbia Univ. Press, pp.193-206. [2] House *et al.* (2000) *Geology* **28**, 707-713. [3] Ueno *et al.* (2001) *Inter. Geol. Rev.* **43**, 196-212. [4] Oehler *et al.* (2006) *Astrobiology* **6**, 838-850.

Linking volcanism and long-wavelength domal swells in Cenozoic Africa

S. NIXON^{1*}, J. MACLENNAN¹, N. J. WHITE¹ AND S. FISHWICK²

¹Bullard Laboratories, University of Cambridge, CB3 0EZ, UK (*correspondence: sn340@cam.ac.uk)

²Department of Geology, University of Leicester, LE1 7RH, UK

The topography of present day Africa is influenced by two different wavelengths of dynamic support. The South African Superplume sits beneath Sub-equatorial Africa and is thought to be supported by a lower mantle thermo-chemical anomaly. On a smaller scale a series of domal swells, 1000km in diameter, occur across the continent. They are characterised by elevated dynamic topography, a positive long-wavelength gravity anomaly and a negative velocity perturbation in a higher mode surface wave tomography model. In addition, where the lithosphere is thinner than 100km, the swells are capped with volcanic products, erupted periodically since ~30 Ma. These include the Cameroon Volcanic line, Hoggar, Tibesti, Darfur, the Ethiopian Plateau and the Kenyan dome. The given relationships suggest the domal swells result from and are supported by upper mantle convection.

The extent of the velocity perturbation is variable. The greatest velocity perturbation being associated with Afar/Ethiopia and smallest perturbations found at the North African swells of Hoggar, Tibesti and Darfur. A database of geochemical data has been assembled for Cenozoic African volcanism of over 3000 samples both by literature search and by new analyses of samples from UK collections. Incompatible trace element ratios from primitive basalts (>7wt% MgO) are used to compare mantle velocity structures with the geochemistry of the products of mantle melting beneath the domal swells. Preliminary work has found the low seismic velocity Afar/Ethiopia region to have shallow melting at high melt fractions (La/Yb ~9) whereas North African swells with higher seismic velocities at 100 km depth, show deeper melting with smaller melt fractions (La/Yb ~30). With further modelling of major, trace and REE data we hope to provide insights into the variation in mantle potential temperature causing the differences in velocity structure and melting processes beneath the topographic swells across the African continent.

Chemistry and mineralogy of aeolian and fluvial supply in shallow-water sediments off Senegal (NW Africa)

J. NIZOU, T.J.J. HANEUBUTH, I. BOUIMETARHAN, C. VOGT, J.B. STUUT AND M. ZABEL

Research Center Ocean Margins, Bremen University, Germany (nizou@uni-bremen.de)

High resolution land related climatic records of the Late Holocene in NW African continental margin are very scarce. The dust material carried by the Trade winds from Sahelian and Saharan regions, and the Senegal River discharges load the continental margin with terrigenous material controlled by climate conditions in the hinterland. Core 9504-3 was retrieved from 43 m water depth in front of the Senegal River mouth. We develop a new approach combining grain-size, elemental distribution and mineralogy employed in parallel with end-member modelling to trace dust and riverine sources through the past and understand how terrigenous components record climate variability.

On the basis of the grain-size distribution of the terrigenous fraction, a splitting was performed providing three subfractions: <2 µm, 2-18 µm and 18-63 µm. Major and trace element contents were measured by XRF powder and ICP-AES, and mineral identification and semi-quantification was performed by X-ray diffraction on each subfraction.

More than 80 % of the total Al and Fe terrigenous bulk sediment content is concentrated in the riverine fraction. Furthermore, despite strong variations, Ti is more abundant in the riverine fraction. Over NW of Africa, due to the scarcity of river draining the continent, Fe and Ti are usually used as dust proxies. Our study displays an alternative interpretation for the terrigenous material deposited off Senegal. K and Si can not be considered as specific proxies.

These results allow us to interpret the XRF core scanner Fe and Al curves as records of the river continental runoff. The correlation between low continental river runoff and period of enhanced dune reactivation in Mali associated with integrated palynological data from the neighbouring Core GeoB 9503-5 confirm these interpretations. The record displays one dry period from 1.9 to 1 cal kyr BP and two main humid periods from 2.7 to 1.9 cal kyr BP and from 1 to 0.7 cal kyr BP. The next step will be to compare this high resolution climatic record to other records in order to establish larger scale teleconnections and understand their mechanisms.

High-precision isotopic compositions of basalts from the last phase of the Hawai'i Scientific Drilling Project

INÈS GARCIA NOBRE SILVA*, DOMINIQUE WEIS AND JAMES S. SCOATES

PCIGR, EOS, University of British Columbia, Canada
(*correspondence: inobre@eos.ubc.ca)

With a total depth of 3464 metres and more than 95% recovery, the Hawai'i Scientific Drilling Project represents the longest sampled stratigraphic sequence of lavas emitted by an oceanic island volcano. In this study, we present Pb, Sr and Nd isotopic compositions of 18 basalts recovered over the final drilling phase (2B) in February 2007. The samples correspond to the last 170 metres of core, with ages > 600 kyr in the stratigraphic record of Mauna Kea.

Isotopically, these samples show the largest range of $^{206}\text{Pb}/^{204}\text{Pb}$ (18.3038–18.6932) and $^{208}\text{Pb}/^{204}\text{Pb}$ (37.9233–38.2703) compared to the rest of the core, especially the samples just above them (3111 to 3326 metres, phase 2B), which showed very restricted isotopic variation. In contrast to the younger basalts that form a broad compositional field in $^{207}\text{Pb}/^{204}\text{Pb}$ - $^{206}\text{Pb}/^{204}\text{Pb}$ space, the older samples analyzed here form a linear array generally characterized by lower $^{207}\text{Pb}/^{204}\text{Pb}$ values for a given $^{206}\text{Pb}/^{204}\text{Pb}$ than the younger lavas. These older lavas extend $^{206}\text{Pb}/^{204}\text{Pb}$ and $^{208}\text{Pb}/^{204}\text{Pb}$ isotopic compositions of Mauna Kea to significantly more radiogenic values, similar to the isotopic compositions shown by “ancestral” Kilauea lavas. In $^{208}\text{Pb}/^{204}\text{Pb}$ - $^{206}\text{Pb}/^{204}\text{Pb}$ space these same samples form two arrays. One Pb array falls within the main Pb isotopic compositional field for Mauna Kea, whereas the other array, composed of samples belonging to the low-SiO₂ group, falls within the “Kea-hi8” trend [1]. This means that a component characterized by high $^{208}\text{Pb}^*/^{206}\text{Pb}^*$ that produced low-SiO₂ contents, was already being sampled early in Mauna Kea's history.

Similar to Mauna Loa, the earlier stages (older lavas) of Mauna Kea volcanism are isotopically more variable than subsequent stages. Overall, the isotopic heterogeneity in Mauna Kea shield lavas can be explained by variable proportions of mixing between three isotopically distinct components intrinsic to the Hawaiian mantle plume during partial melting and formation of the basaltic magmas. These components are: the more radiogenic “Kea” or “Hilina” component [2], a high $^{208}\text{Pb}^*/^{206}\text{Pb}^*$ (producing low-SiO₂ basalts) component, and a component with less radiogenic Pb isotopic compositions.

[1] Eisele *et al.* (2003) *G3* **4**, 1-32. [2] Kimura *et al.* (2006) *JVGR* **151**, 51-72.

Simulation of the nucleation and growth of solid solutions in aqueous solutions

C. NOGUERA^{1*}, B. FRITZ², Y. AMAL² AND A. CLEMENT²

¹INSP, CNRS-UPMC, Paris, France

(*correspondence: claudine.noguera@insp.jussieu.fr)

²CGS, CNRS-ULP, Strasbourg, France

(bfritz@illite.u-strasbg.fr)

Nucleation and growth of solid-solutions in aqueous media (SS/AS) are related to a number of societal questions such as contamination of soils and ground-waters, global element cycles, hydrothermal ore-forming processes, etc. However, their full simulation, including kinetic effects in the first steps of their formation, still remains a challenge.

This is the purpose of the present work, which extends our previous studies of minerals of fixed composition [1-4]. Here, we model precipitation processes for ideal SS of the A_{1-x}B_xC type, with variable composition x. The model is based on the classical nucleation theory, on a size-dependent (algebraic) growth law allowing growth, resorption and ripening of particles simultaneously, and on conservation laws akin to a thermodynamically closed system. The composition dependence of critical nuclei and growing particles has been assumed to follow laws similar to those of binary droplet condensates, precipitates in metallic alloys and segregation at alloy surfaces.

The model has been embedded in the geochemical code Nanokin that we have elaborated. We will present results for the precipitation of solid-solutions whose end-members have either similar or very different solubilities, thus allowing distinct ion partitionings and composition profiles.

Support of the French ANR-PNANO 2006 (project “SIMINOX” 0039) is acknowledged.

[1] C. Noguera, B. Fritz, A. Clément & A. Baronnet, (2006) *J. Cryst. Growth* **297**, 180-186. [2] C. Noguera, B. Fritz, A. Clément & A. Baronnet (2006) *J. Cryst. Growth* **297**, 187-198. [3] B. Fritz, A. Clément, Y. Amal & C. Noguera, (2007) “NANOKIN, a geochemical computer model for dissolution, nucleation & growth in aqueous solutions” (in preparation) [4] B. Fritz, A. Clément, Y. Amal & C. Noguera, this volume.

Multielemental determination of GEOTRACES key trace metals by column concentration and ICP-MS

KAZUHIRO NORISUYE*, SHOUHEI URUSHIHARA,
SEIJI NAKATSUKA, TOMOHIRO KONO¹, ERI HIGO,
TOMO HARU MINAMI AND YOSHIKI SOHRIN

Institute for Chemical Research, Kyoto University, Uji, Kyoto
611-0011, Japan

(*correspondence: knorisue@inter3.kuicr.kyoto-u.ac.jp)

Al, Mn, Fe, Cu, Zn and Cd are assigned as GEOTRACES key trace metals and their global ocean distributions are going to be determined through a number of cruises. A simple, rapid, accurate and precise method is invaluable for the GEOTRACES section study. However, it has been difficult to determine these metals at the same time due to contamination and interference from major constituents. This work introduces a novel method of solid phase extraction for determination of Al, Mn, Fe, Co, Ni, Cu, Zn, Cd, and Pb in seawater by inductively coupled plasma-mass spectrometry (ICP-MS) [1].

The trace metals were collected from 120 mL of seawater using a column of ethylenediaminetriacetic acid-immobilized vinyl polymer resin and eluted with 15 mL of 1 M HNO₃. Then Mn and Fe in the eluate were measured by ICP-MS (ELAN DRC II, Perkin-Elmer) using a DRC mode and the other metals were measured using a normal mode.

By the procedure, the trace metals were collected quantitatively, while >99.9% of alkali and alkaline earth metals in seawater were removed. For each trace metal, the procedural blank was <16% of the mean concentration in the open-ocean, and the precision was <9% in RSD. Moreover, this method was free from contamination even in a non-clean room laboratory. Our values for the trace metals in the certified reference materials of seawater NASS-5 and nearshore seawater CASS-4 agreed with the certified values (except that there is no certified value for Al). This method was also successfully applied to the reference materials of open-ocean seawater produced by the SAFe program. Our Fe concentrations were 5.9 ± 0.7 ng/kg for surface water (S1) and 50.4 ± 2.9 ng/kg for deep water (D2), being in agreement with the interlaboratory average of 5.4 ± 2.4 ng/L and 50.8 ± 9.5 ng/L, respectively. The data for other metals were oceanographically-consistent.

[1] Sohrin *et al.* (submitted) *Anal. Chem.*

Microbial catalysis of jarosite formation under environmentally relevant AMD conditions

KELSEY L.I. NORLUND AND LESLEY A. WARREN

School of Geography and Earth Sciences, McMaster
University, Hamilton, ON, Canada

(norlunkl@mcmaster.ca, warrenl@mcmaster.ca)

The formation of jarosite in acid mine drainage (AMD) accompanies microbial catalysis of S oxidation associated with reduced sulfidic minerals such as pyrite and pyrrhotite. Little documented information on jarosite formation under environmentally relevant conditions currently exists, despite its increasing interest as a tracer of water and potentially life on other planets, and for mine mitigation strategies. Such information is critical for more accurate understanding of acid/metal leachate generation in AMD systems, and more robust biosignatures for the search for life elsewhere. The objective of this study was to examine the conditions for jarosite formation associated with microbial oxidation of pyrrhotite-rich slurry by a natural AMD microbial enrichment under constrained laboratory conditions. Sterilized slurry (>60% pyrrhotite) from the Xstrata Nickel concentrator (Onaping, ON) was inoculated with the natural enrichment and run parallel to abiotic controls at an initial pH of 6 in batch experiments. Samples were collected at predetermined pH values for sulphate and mineralogical analyses to identify initiation of jarosite formation. Results indicate that microbial processing of the slurry was required for acid generation and mineralogical changes accompanied the pH decrease (XRD). These environmental AMD microbial enrichments catalyzed jarosite formation at pH values of 3.5 in contrast to literature reports of a maximum pH of 3 for jarosite formation. These mineralogical changes will be discussed in conjunction with observed microbial S processing and characterization of the environmental enrichment consortia.

Age and origin of Apollo 16 feldspathic fragmental breccias

M.D. NORMAN¹ AND R.A. DUNCAN²

¹RSES, Australian National University, Canberra ACT 0200 AU (*correspondence: marc.norman@anu.edu.au)

²COAS, Oregon State University, Corvallis, OR 97331 USA (rduncan@coas.oregonstate.edu)

In order to improve our understanding of lunar impact history and development of crustal terranes on the Moon, we measured ⁴⁰Ar-³⁹Ar ages and major+trace element compositions of anorthositic and melt breccia clasts from Apollo 16 feldspathic fragmental breccias 67016 and 67455. These breccias represent the Descartes terrane, a regional, highly feldspathic unit of the central nearside highlands generally considered to be ejecta from the nearby Nectaris basin. The goal of this work is to place better constraints on the emplacement age and provenance of the Descartes breccias.

Four anorthositic clasts from 67016 yielded well-defined ⁴⁰Ar-³⁹Ar ages ranging from 3842±19 to 3875±20 Ma (relative to MmHb-1=513.9 Ma). Replicate analyses of these clasts all agree within measurement error. The weighted mean age for these clasts is 3862±12 Ma (95% conf., n=7, MSWD=1.3). There is little evidence for older components in the Ar spectra of these clasts. In contrast, fragment-laden melt breccia clasts from 67016 yield apparent ages of 4.1 to 4.2 Ga and evidence of even older material (to 4.5 Ga) in the high-T fractions. The 67455 clasts have more variable spectra with evidence for low-T Ar loss. Plateau ages of 3801±29 to 4012±21 Ma for three anorthositic clasts (weighted mean 3935±86 Ma), and 3987±21 Ma for one melt breccia clast were obtained.

Diagnostic trace element ratios (Sr/Ba, Ti/Sm, Sc/Sm) in these clasts all change systematically to lower values with increasing incompatible element abundance. These trends are consistent with mixing of ferroan anorthositic rocks with KREEP and/or Mg-suite components.

An assembly age of 3862 Ma based on the 67016 anorthositic clasts would be younger than Serenitatis and identical with the accepted age of the Imbrium basin. Trace element compositions of clasts in the Descartes breccias suggest a provenance in the Procellarum-KREEP terrane. The combination of age and provenance constraints implies that the Descartes breccias formed during the Imbrium event or by local craters rather than as Nectaris ejecta. Older ages for coexisting melt breccia clasts probably reflect incomplete degassing rather than the emplacement age of the breccias.

Water chemistry of lake inlets and outlet as a predictor of sediment characteristics and internal cycling of phosphorus

S. NORTON^{1*}, A. AMIRBAHMAN¹, T. WILSON¹ AND J. KOPÁČEK²

¹University of Maine, Orono, ME 04469-5790, USA (*correspondence: Norton@Maine.edu)

²Biology Centre ASCR, HBI, České Budějovice, C.R

Chemical characteristics of lake sediment determine if PO₄ is released during anoxia. The reductive dissolution of hypolimnetic sedimented Fe(OH)₃ is not accompanied by release of PO₄ if Psenner sequential extractions [1] reveal, (1) the molar ratio of Al_{NaOH25}:Fe_{bicarbonate/dithionite} is >3; or (2) the molar ratio of Al_{NaOH25}:P_(H2O + bicarbonate/dithionite) is >25 [2]. The extractable Al and Fe hydroxides strongly adsorb PO₄. We have evaluated chemistry of inlets and outlets for four lakes, and estimated input and output fluxes of Al, Fe, Mn, and P, based on a combination of (1) numerical averages of chemistry of multiple seasonally-distributed samples, (2) chemical characterization of high discharge events, and (3) approximate areas drained by the inlets. Concentrations of total acid-soluble, and total dissolved and organically-bound Al, Fe, Mn, P, and DOC are typically reduced 75 to 90% during water's passage through the lake. Photodegradation of organically-bound metals apparently releases inorganic species which precipitate as hydroxide and scavenge PO₄. Psenner-extractable proportions of total Al, Fe, Mn, and P in the sediment are approximately the same as are lost during lake residence time, based on inlet and outlet chemistry. We estimated the sedimentation rate of Al(OH)₃, Fe(OH)₃, Mn(hydroxide?), and P to the profundal areas of the lakes with ²¹⁰Pb-dated cores [3]. These rates are similar to the rates at which Al, Fe, Mn, and P are removed from the lake water column. Thus, comparison of inlet and outlet stream chemistry yields inferences about sediment chemistry, and enables predictions about P retention by lake sediment.

[1] Psenner *et al.* (1988) *Hydrobiologia* **170**, 91-101.

[2] Kopáček *et al.* (2005) *Environ. Sci. Technol.* **39**, 8784-8789. [3] Norton *et al.* (in press) *Sci. Tot. Environ.*

$\delta^{13}\text{C}$ values of carbon forms in vertical *Sphagnum* peat profiles in different climatic zones

MARTIN NOVAK*, IVA JACKOVA, EVA PRECHOVA,
FRANTISEK BUZEK, PETRA PACHEROVA AND LUCIE
ERBANOVA

Czech Geological Survey, Geologicka 6, 152 00 Prague 5,
Czech Republic
(*correspondence: martin.novak@geology.cz)

Peatlands accumulate one third of the world's soil carbon. During climatic warming, higher emanations of greenhouse gases, accompanying thinning of peat deposits, may lead to further temperature increases. The formation of CO_2 and CH_4 during peat decomposition depends on organic matter quality. We studied the relationship between C cycling in peatlands and climate using peat cores collected in the Czech Republic (Central Europe) and northern Sweden (Northern Europe). The mean annual temperatures were 7.2 and 4.0 °C, respectively. Preliminary data indicated that bulk C can become both isotopically lighter and heavier downcore, but it is not known which C species are responsible for these isotope shifts. Therefore we sequentially extracted and quantified the following organic C forms in peat: soluble fats, oils and waxes; soluble carbohydrates; soluble phenolics; total hot-water solubles; holocellulose; α -cellulose; hemicellulose; lignin; and acid-soluble carbohydrates. Seven most abundant C forms were analysed also isotopically. So far, $\delta^{13}\text{C}$ data were obtained for two sites with a positive downcore $\delta^{13}\text{C}$ shift in bulk peat. At Velke Darko (the warmer site, Czech Republic), three types of vertical $\delta^{13}\text{C}$ trends were observed: throughout the profile, $\delta^{13}\text{C}$ of lipids was the lowest in the system, fluctuating around -30 per mil. At a depth of 30 cm, $\delta^{13}\text{C}$ of lipids was 8 per mil lower than that of cellulose. $\delta^{13}\text{C}$ of all forms of cellulose, carbohydrates and phenolics overlapped, increasing smoothly downcore from -27 to -22 per mil. $\delta^{13}\text{C}$ of lignin, also increasing downcore, was off-set relative to cellulose by 2 per mil to more negative values, but never became as low as $\delta^{13}\text{C}$ of lipids. At Stor Amyran, a site located near the Polar Circle (Sweden), $\delta^{13}\text{C}$ of both lipids and lignin were more negative compared to Velke Darko. At the same time, $\delta^{13}\text{C}$ of cellulose at Stor Amyran was higher than $\delta^{13}\text{C}$ of cellulose at Velke Darko. The northern site showed less steep increase in $\delta^{13}\text{C}$ of bulk peat with increasing depth. We propose that this pattern is a result of slower peat decomposition at the northern site.

Fluid inclusions in archean ultrahigh-temperature metamorphic BIF of the Ukrainian Shield (East European craton, Russia)

M.A. NOVIKOVA

Institute of Experimental Mineralogy, Russian Academy of
Sciences, Chernogolovka, Moscow district, Russia
(nov@iem.ac.ru)

Fluid inclusions have been studied in high-grade BIF of the Ukrainian Shield. The fluid inclusions comprise CO_2 -rich and less abundant nitrogen-methane, salt-bearing aqueous and pure aqueous varieties. Two generations of CO_2 -rich inclusions are distinguished. First generation (FL I) inclusions are represented by primary inclusions of high density (1.142 g/cm³) with very low Th min: -46.6 °C. The melting temperatures (Tm) of these inclusions vary from 56.7°C to -59.8°C. Some depression of Tm in comparison with -56.6 °C for pure carbon dioxide is caused by an admixture of additional components, as is supported by the Raman spectroscopy that detected methane. Most density inclusions are grouped in the cores of quartz grains. Second generation (FL II) inclusions are represented by pseudosecondary CO_2 -rich inclusions with Th min of -29.3 °C (density 1.073 g/cm³). Their melting temperature varies from -56.6 to -58.2°C. These are located along healed cracks most usually in the periphery of quartz grains. Different generations of the CO_2 -rich fluid inclusions indicate the multistage metamorphism in the region. N_2 - CH_4 inclusions are primary or rarer pseudosecondary. They are clustered as separate groups in cores of quartz grains and less frequently at grain margins. Their Th vary from -128.4 to -154.5°C. Such low Th values can testify to some admixture of methane in nitrogen (3-35 mol % CH_4). The primary N_2 - CH_4 inclusions are often associated with high-density CO_2 -rich inclusions of the first generation. The high-density inclusions FL1 were revealed in BIF, which often contains clino- and orthopyroxenes with exsolution textures. Using the reintegrated compositions of the primary clinopyroxene and pigeonite and the Lindsley [1] geothermometer it was found the ultrahigh temperature ($\geq 930^\circ\text{C}$) of the peak metamorphism. The peak metamorphic pressure of the BIF was estimated as 9-10 kbar at depth 36-40 km using isochore of the CO_2 -rich inclusions with highest density and calculated temperature.

[1] Lindsley (1983) *American Mineralogist* **68**, 477-493.

Laser ablation Pt-Re-Os analysis and chronometry of mantle-derived minerals

G.M. NOWELL¹, J.A. COGGON¹, D.G. PEARSON¹,
S.W. PARMAN¹, E. HANSKI² AND P. TUISKU²

¹NCIET, Dept. Earth Sciences, University of Durham, Durham DH1 3LE (g.m.nowell@durham.ac.uk)

²Department of Geology, University of Oulu, Linnanmaa Door K, FIN-90014, Oulu, Finland

The Re-Os isotope system has proved an extremely important tracer and chronometer of mantle processes over the past two decades. In contrast, the Pt-Os isotope system has been far less utilised, due to the difficulties of analysing the low abundance ¹⁸⁶Os and ¹⁹⁰Pt isotopes and the long half-life of ¹⁹⁰Pt. Despite this the potential of the Pt-Os system in mantle geochemistry is clear and is ripe for further development [eg 1-2]. Applications of Pt-Os chronometry have been few but advances in mass spectrometry have allowed us to develop a method for rapid (40 seconds) and simultaneous acquisition of Re-Os and Pt-Os isotope data on individual Platinum Group Alloys (PGAs) by laser ablation MC-ICP-MS [3].

There is sufficient variation in Pt/Os ratios within mantle-derived micro-phases to exploit as a chronometer and so we have applied this to dating PGAs associated with ophiolite complexes, which have hitherto have been extremely difficult to date. Preliminary Pt-Os isotope data for detrital PGA grains from Borneo will be presented that yield a Pt-Os isochron age of 207.6±6.5Ma (MSWD 1.5), close to the best estimates for the Meratus ophiolite from which the grains are thought to derive. Calculated initial ¹⁸⁶Os/¹⁸⁸Os ratios are also entirely consistent with mantle values. Obvious caution must be exercised when interpreting isochron ages based on detrital PGAs which may be temporally or genetically unrelated and could be derived from multiple parent bodies. This ambiguity can be avoided by dating individual PGA grains containing exsolved phases or multi-mineral intergrowths. Data will also be presented for both multi-grain and the first ever single-grain Pt-Os ages for PGA grains associated with the Central Lapland Greenstone Belt (CLGB). We will also illustrate that where Re-Os and Pt-Os ages can be obtained on the same PGA grain or group of grains there is always an age discordance, with Re-Os always being the younger. This will be shown to be an analytical limitation of laser ablation Re-Os dating. Nonetheless, it is clear that Pt/Os chronometry has widespread application to the dating of mantle phases and rocks.

[1] Brandon *et al.* (1998) *Science* **280**, 1570-1573. [2] Luguet *et al.* (2008) *Science* **319**, 453-456. [3] Nowell *et al.* (2008 in press) *Chem. Geol.*

Insights into lithospheric mantle beneath Patagonia

TH. NTAFLLOS^{1*}, A.E. BJERG² AND P. ALIANI²

¹Dept. of Lithospheric Researches, University of Vienna, Austria (*correspondence: ntaflot9@univie.ac.at)

²Ingeosur-Conicet and Dept. of Geology-UNS, Bahia Blanca, Argentina (ebjerg@uns.edu.ar)

The lithospheric mantle beneath Patagonia (PTG), as can be inferred from studies on mantle xenoliths, is highly inhomogeneous. In northern PTG the majority of mantle xenoliths show evidences of cryptic metasomatism, except those from Comallo that have traces of amphibole. In contrast, in southern PTG, the lithospheric mantle beneath Gobernador Gregores (Gb) is heavily modal metasomatized by abundant amphibole and/or phlogopite.

In northern PTG, gt-bearing peridotites occur in Prahuaniyeu (Pr), close to the NW margin of the Somoncura large igneous province. They are characterized by high T = 1100–1230 °C and low P = 19.5–24 kbar. Zr is enriched in garnets from fertile gt-peridotites and depleted in garnets from residual gt-peridotites. Ti-content in gt shows no variations and appears to be decoupled from the behaviour of Zr. The cpx trace element patterns from gt-peridotites always have negative Zr anomaly but no Ti anomaly. In contrast, worldwide cpx from sp-peridotites generally have negative Ti anomaly in PM-normalized trace element patterns. Therefore the presence or absence of negative Ti anomaly could reveal whether or not the peridotites have experienced melting processes in the gt-peridotite field. Zr^{Dcpx/Dgt} ratios of about 1 from a group of Pr gt-peridotites cannot be explained by simple melting processes and require introduction of melts causing cryptic metasomatism responsible for Zr enrichments in cpx.

These gt-peridotites have experienced up to 8% partial melting and slight cryptic metasomatism under low P-high T conditions, suggesting an ascending mantle plume.

The heavily metasomatized sp-peridotites from Gb have abundant melt pockets that according to mass balance calculations represent breakdown and melting of amphiboles with minor contribution of external melts. Amph, glass and partly cpx are strongly enriched in incompatible elements. Mantle xenoliths from the southern PT localities Tres Lagos and Cerro Redondo, south of Gb, are more depleted in basaltic components and suggest a lithospheric mantle at this region practically unaffected by metasomatic processes. Those differences and, the fact that the crust at Gb is a metamorphic unit of latest Proterozoic age whereas at the other two localities it is younger (Palaeozoic), suggest a boundary between two different micro tectonic plates.

Does Iron dissociation from siderophores lead to Iron isotope fractionation?

JOCHEN NUESTER¹, LAURA J LIERMANN²,
LAURA E WASYLENKI³, ARIEL D ANBAR⁴ AND
SUSAN L BRANTLEY⁵

¹Penn State University, University Park, PA 16801

(*correspondence: jun5@psu.edu) (lj18@psu.edu)

²Earth and Planetary Sciences, ASU, Tempe, AZ 85287

(laura.wasylenki@asu.edu, anbar@asu.edu)

³EESI, Penn State University, University Park, PA 16801

(brantley@essc.psu.edu)

Over the last decade iron isotope geochemistry has increased our potential to trace the geochemical cycling of iron, but the mechanisms responsible for iron cycling in subsurface environments are poorly understood and correlation of iron isotope signals to distinct subsurface processes is difficult to show. As the mechanisms which govern iron isotope fractionation in natural ecosystems are under debate, we will focus our research on the poorly constrained process of iron dissociation from siderophores and other iron chelators.

Siderophores are low molecular weight organic ligands released by bacteria or fungi to increase the bioavailability of iron. Even though the high stability of iron siderophore complexes suggests the chelated Fe(III) is largely unavailable for inorganic processes, we observed that Fe(III) can be dissociated by a reductive mechanism using ascorbic acid.

Initial abiotic kinetic experiments show distinct variations in the kinetics of iron dissociation from ferric acetohydroxamic acid (Fe-AHA₃), ferric EDTA (Fe-EDTA⁻), and ferrioxamine B (Fe-DFOB⁺). The pseudo first order rate constants (*k'*) vary four orders of magnitude with *k'*(Fe-AHA₃) > *k'*(Fe-EDTA⁻) > *k'*(Fe-DFOB⁺) resulting in half-lives from seconds for Fe-AHA₃, to minutes for Fe-EDTA⁻, and to days for Fe-DFOB⁺. The displacement of iron from Fe-DFOB⁺ can be accelerated in the presence of Ga, which reduces the half-life to hours. Furthermore, the presence of a catalyst like oxalic acid and a competing ligand like EDTA can accelerate this dissociation process as well.

In order to understand iron cycling in natural environments we will extend our studies on possible iron fractionation during the abiotic reductive displacement of Fe(III). Such iron isotope signals could improve our understanding of iron cycling in terrestrial subsurface environments. Initial measurements indicate that preferentially light iron is removed from the ligands.

Augustine Volcano: Mg, Cr, & Ni-rich; LILE, REE and HFSE-poor

C.J. NYE^{1*}, M.L. COOMBS², J. LARSEN³, P. IZBEKOV³,
M. TILMAN³ AND C. CAMERON¹

¹AVO, Alaska Geol & Geophys Surveys, Fairbanks, Alaska

(*correspondence: cnye@giseis.alaska.edu)

²AVO, US Geological Survey, Anchorage Alaska

³AVO, University of Alaska Fairbanks Geophysical Institute, Fairbanks, Alaska

Augustine is a ~1300m tall, active volcano near the eastern end of the Aleutian Arc. Each of five major eruptions in the past century has erupted banded and hybridized crystal-rich andesite spanning ~56 to ~64% SiO₂. Basalt and rhyolite are restricted to late Pleistocene time. A continuum of lavas spanning the entire basalt-rhyolite compositional range of the volcano is notably absent, and distinguishes Augustine from many other Aleutian arc volcanoes.

Augustine is among several Aleutian arc volcanoes sharing the characteristics, relative to the rest of the arc, of high Mg, Cr, Ni, Mg# and low LILE, REE, HFSE, U, Th, Pb.

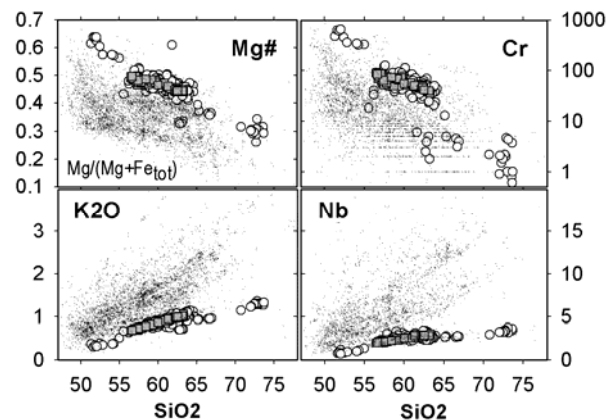


Figure 1: Compositions of Augustine lavas compared to other Aleutian Arc lavas (dots). Filled squares are from the 2006 eruption, open circles are from all pre-2006 samples.

The low concentrations of incompatible elements reflect a span of concentrations that is half or less of that of typical Aleutian suites (relative to base-level) as well as low initial concentrations. This, and the lack of Eu anomalies in evolved rocks severely limits petrogenetic relationships involving plagioclase-dominated fractionation. The chemical, petrographic, and mineralogic data suggest petrogenesis is a complex process involving deep crustal or near-Moho crystallization, entrainment of crystalline residues from previous magma batches, and mixing.